JOC Article

Diastereoselective Synthesis of 2-Amino-4-phosphonobutanoic Acids by Electrophilic Substitution and Tin−Peterson Olefination of Bis-lactim Ethers Derived from *cyclo*-[L-AP4-D-Val]

María C. Fernández,† Aniana Díaz, Juan J. Guillín, Olga Blanco, María Ruiz,* and Vicente Ojea*

Departamento de Química Fundamental, Facultade de Ciencias, Universidade da Coruña, Campus da Zapateira s/n, 15071 A Coruña, Spain

ojea@udc.es; ruizpr@udc.es

Received May 25, 2006

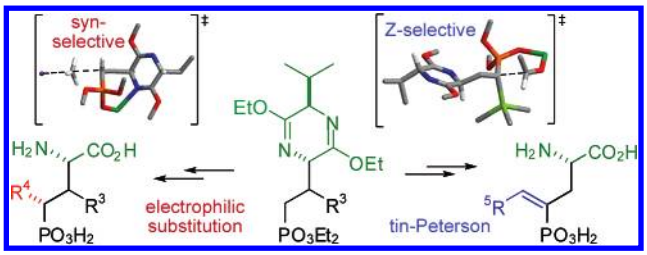

Electrophilic substitutions on lithiated Schöllkopf's bis-lactim ethers derived from *cyclo*-[L-AP4-D-Val] take place regio- and stereoselectively at the α-position of the phosphonate ester. Subsequent olefination of α-silyl-, α-phosphoryl-, and α-stannyl-stabilized phosphonate carbanions give rise exclusively to vinylphosphonates. Both processes allow a direct and stereoselective access to a variety of 4-substituted and 3,4-disubstituted 2-amino-4-phosphonobutanoic acids (AP4 derivatives) in enantiomerically pure form that may be useful tools for characterizing the molecular pharmacology of metabotropic glutamate receptors (mGluRs) of group III. The relative stereochemistry was assigned from X-ray diffraction analyses or NMR studies of 1,2-oxaphosphorinane and other cyclic derivatives. In accordance to density functional theory (DFT) calculations, the syn-selectivity in the electrophilic substitutions may originate from the intervention of seven- and eight-membered chelate structures in which the bis-lactim ether moiety shields one of the faces of the phosphonate carbanion. DFT calculations for the tin−Peterson olefination of α-stannyl stabilized phosphonate carbanions indicate that rate and selectivity are determined in the initial carbon−carbon bond formation step where the unlike transition structures leading to (*Z*)-vinylphosphonates are favored both in the gas phase and in THF solution.

Introduction

Glutamate is the most important excitatory neurotransmitter in the central nervous system (CNS).[1] After being released from the presynaptic terminal, glutamate diffuses across the synaptic cleft and binds to its receptors on the dendrites of the postsynaptic neurons. Glutamate receptors (GluRs) are involved in a variety of physiological functions, including neuronal plasticity, long-term potentiation of synaptic activity, and memory as well as in acute or chronic pathological processes such us brain ischemia, pain, psychiatric disorders, and neurodegenerative diseases. Thus, GluRs are valuable therapeutic targets.[2] GluRs are categorized into two main classes: ionotropic glutamate receptors (iGluRs),[3] which are ligand-gated ion channels, and metabotropic glutamate receptors (mGluRs), which are G-protein-coupled receptors involved in the regulation of glutamate release and the modification of the postsynaptic excitability to glutamate. There are currently eight known subtypes of mGluRs, which can be classified into three subgroups (groups I, II, and III) according to pharmacological

† Present address: Lilly S.A., Alcobendas, Madrid, Spain.

(1) (a) *CNS Neurotransmitters and Neuromodulators: Glutamate;* Stone, T. W. Ed.; CRC: Boca Raton, Florida, 1995. (b) Parthasarathy, H. S., Ed. *Nature* **1999**, *399* (Suppl.), A1−A47. (c) Ozawa, S.; Kamiya, H.; Tsuzuki, K. *Prog. Neurobiol.* **1998**, *54*, 581−618.

(2) Bräuner-Osborne, H.; Egebjerg, J.; Nielsen, E. O.; Madsen, U.; Krogsgaard-Larsen, P. *J. Med. Chem.* **2000**, *43*, 2609−2645.

(3) *The Ionotropic Glutamate Receptors;* Monahan, D. T., Wenthold, R. J., Eds.; Humana: Totowa, New Jersey, 1997.

10.1021/jo061072x CCC: $33.50
Published on Web 08/11/2006

CHART 1. Selective Ligands for the MGluRs of Group III

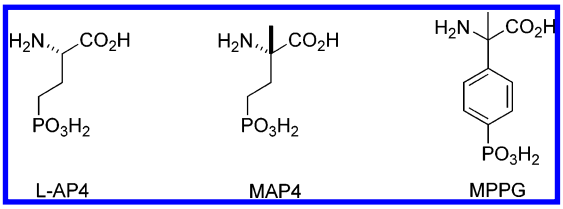

properties, signal transduction mechanisms, and sequence similarity. Among the receptors of group III, mGluR4, mGluR7, and mGluR8 are presynaptically localized and inhibit the release of neurotransmitters, whereas mGluR6 receptors are exclusively expressed by ON bipolar cells in the retina and play an important role in the amplification of visual inputs. mGluRs of group III are characterized by their response to several phosphonic amino acid derivatives.[4] They are selectively activated by L-2-amino-4-phosphonobutanoic acid (L-AP4, see Chart 1) and competitively antagonized by α-methylated derivatives of L-AP4 (MAP4) and 4-phosphonophenylglycine (MPPG).

Elucidation of the role that mGluRs play in the normal and pathological functioning of the CNS still depends on the development of more potent and subtype-selective pharmacological agents.Therefore, there is considerable interest in the development of new synthetic methodologies for the preparation of enantiomerically pure AP4 derivatives that may result in useful tools for determining the requirements for receptor binding and physiological responses at mGluRs of group III.

Three major strategies have been devised for the preparation of AP4 derivatives. Phosphites have been reacted with functionalized carbonyl compounds that were subsequently converted to amino acids via Strecker reaction,[5] or have been reacted with halides,[6] triflates,[7] or carbonyl functionalities[8] located at the side chain of α-amino acid derivatives. Alternative synthesis have relied on glycine enolate equivalents for the alkylation of,[9] 1,3-dipolar cycloaddition to,[10] or conjugate addition to[11] suitable functionalized phosphonates. In this area, we have shown that conjugate additions of lithiated Schöllkopf's bis-lactim ethers **5** to vinylphosphonates **6** with alkyl, aryl, or functionalized substituents at the *β*-position allow a direct and stereocontrolled access to 3-substituted 2-amino-4-phosphonobutanoic acids **1** with 2,3-syn or 2,3-anti configurations (see Scheme 1).[12] Nevertheless, the scope and the stereoselectivity of the corresponding additions to α-substituted vinylphosphonates **8** were found to be reduced, seriously compromising the utility of this methodology for the synthesis of 4-substituted AP4 derivatives.

To develop an alternative approach to this class of compounds, we decided to investigate the electrophilic substitution processes on the bis-lactim ethers **2**, derived from *cyclo*-[L-AP4-D-Val]. On the basis of its potential role as first intermediates resulting from the additions of **5** to vinylphosphonates **6**, phosphonate carbanions **3** should be accessible by treatment of **2** with an adequate base. Subsequent trapping of **3** with different electrophilic reagents could give rise, selectively, to 2′-substituted bis-lactim ether intermediates **4**.[13] We also envisaged that the electrophilic substitutions on **3** with phosphoryl, silyl, or stannyl groups could be followed by Wadsworth−Emmons or Peterson-like olefinations of carbonyl compounds and could give rise to vinylphosphonates **7** as precursors of 4-alkylidene AP4 derivatives. Thus, in this paper we report in full detail the application of such a methodology to the synthesis of a variety of enantiomerically pure 4-substituted and 3,4-disubstituted AP4 derivatives **1**,[14] which may be useful for characterizing the molecular pharmacology of the mGluRs of group III.

Results and Discussion

Throughout this article, bis-lactim ethers, amino esters, amino acids, and their derivatives will be referred to with numerals followed by two letters, according to the central key depicted in Chart 2. Numerals describe generic stereoisomers, and letters are used to distinguish the identity of the substituents R^3 and R^4 (or R^5) at positions 3 and 4 (or 5) of the targeted AP4 derivatives.

Electrophilic Substitutions of Bis-lactim Ethers Derived from *cyclo*-[L-AP4-D-Val]. We first studied the electrophilic substitution processes on the bis-lactim ether **11aa**, which was derived from *cyclo*-[L-AP4-D-Val]. Preparation of this unsubstituted precursor was achieved by adaptation of the procedure reported by Shapiro et al.[11a] for the synthesis of the *O,O*-diallyl phosphonate derivative. Thus, addition of an equimolar solution of bromoethylphosphonate **9** containing 5% of vinylphosphonate **10** to the lithium salt **5** in THF at −78 °C afforded bis-lactim ether **11aa** in 85% yield virtually free of the 2,5-cis diastereoisomer (see Scheme 2).[15] The exceptionally high 2,5-trans selectivity achieved in this "alkylation" can be understood considering that the addition of the lithium salt **5** to vinylphos-

(4) (a) Filosa, R.; Marinozzi, M.; Constantino, G.; Brunsgaard Hermit, M.; Thomsen, C.; Pellicciari, R. *Bioorg. Med. Chem.* **2006**, *14*, 3811−3817. (b) Swanson, C. J.; Bures, M.; Johnson, M. P.; Linden, A.-M.; Monn, J. A.; Schoepp, D. D. *Nat. Rev. Drug Discovery* **2005**, *4*, 131−144. (c) Moldrich, R. X.; Chapman, A. G.; De Sarro, G.; Meldrum, B. S. *Eur. J. Pharmacol.* **2003**, *476*, 3−16. (d) De Blasi, A.; Conn, P. J.; Pin, J.-P.; Nicoletti, F. *Trends Pharmacol. Sci.* **2001**, *22*, 114−120. (e) Conn, P. J.; Pin, J.-P. *Annu. Rev. Pharmacol. Toxicol.* **1997**, *37*, 205−237.

(5) (a) Crooks, S. L.; Robinson, M. B.; Koerner, J. F.; Johnson, R. L. *J. Med. Chem.* **1986**, *29*, 1988−1995. (b) Johnson, R. L.; Rao, K. S. S. P. *Bioorg. Med. Chem. Lett.* **2005**, *15*, 57−60. See also 4a and Massey, S. M.; Monn, J. A.; Valli, M. J. U.S. Patent 5,958,960, 1999.

(6) (a) Nair, S. A.; Lee, B.; Hangauer, D. G. *Synthesis* **1995**, 810−814. (b) Ma, D.; Ma, Z.; Jiang, J.; Yang, Z.; Zheng, C. *Tetrahedron: Asymmetry* **1997**, *8*, 889−893. (c) Bessieres, B.; Schoenfelder, A.; Verrat, C.; Mann, A.; Ornstein, P.; Pedregal, C. *Tetrahedron Lett.* **2002**, *43*, 7659−7662. See also: Hanrahan, J. R.; Taylor, P. C.; Errington, W. *J. Chem. Soc., Perkin Trans. 1* **1997**, 493−502.

(7) (a) Berkowitz, D. B.; Eggen, M.-J.; Shen, Q.; Shoemaker, R. K. *J. Org. Chem.* **1996**, *61*, 4666−4675. (b) Amori, L.; Costantino, G.; Marinozzi, M.; Pellicciari, R.; Gasparini, F.; Flor, P. J.; Kuhn, R.; Vranesic, I. *Bioorg. Med. Chem. Lett.* **2000**, *10*, 1447−1450.

(8) (a) Wiemann, A.; Frank, R.; Tegge, W. *Tetrahedron* **2000**, *56*, 1331−1337. (b) Perich, J. W. *Int. J. Pept. Protein Res.* **1994**, *44*, 288−294.

(9) (a) Soloshonok, V. A.; Belokon, Y. N.; Kuzmina, N. A.; Maleev, V. I.; Svistunova, N. Y.; Solodenko, V. A.; Kukhar, V. P. *J. Chem. Soc., Perkin Trans. 1* **1992**, 1525−1529. (b) Schöllkopf, U.; Busse, U.; Lonsky, R.; Hinrichs, R. *Liebigs Ann. Chem.* **1986**, 2150−2163.

(10) (a) Casas, J.; Grigg, R.; Nájera, C.; Sansano, J. M. *Eur. J. Org. Chem.* **2001**, 1971−1982. (b) Matoba, K.; Yonemoto, H.; Fukui, M.; Yamazaki, T. *Chem. Pharm. Bull.* **1984**, *32*, 3918−3925.

(11) (a) Shapiro, G.; Buechler, D.; Ojea, V.; Pombo-Villar, E.; Ruiz, M.; Weber, H.-P. *Tetrahedron Lett.* **1993**, *34*, 6255−6258. (b) Minowa, N.; Hirayama, M.; Fukatsu, S. *Tetrahedron Lett.* **1984**, 25, 1147−1150.

(12) (a) Ruiz, M.; Fernández, M. C.; Díaz, A.; Quintela, J. M.; Ojea, V. *J. Org. Chem.* **2003**, *68*, 7634−7645. (b) Ojea, V.; Ruiz, M.; Shapiro, G.; Pombo-Villar, E. *J. Org. Chem.* **2000**, *65*, 1984−1995.

(13) For previous asymmetric synthesis of phosphonic acids using phosphoryl-stabilized carbanions, see: (a) Denmark, S. E.; Chen, Ch. T. *J. Am. Chem. Soc.* **1995**, *117*, 11879−11897 and references therein. (b) Hanessian, S.; Bennani, Y. L. *Tetrahedron Lett.* **1990**, *31*, 6465−6468.

(14) Part of this work already was presented as preliminary communications: (a) Ruiz, M.; Ojea, V.; Quintela, J. M.; Guillín, J. J. *Chem. Commun.* **2002**, 1600−1601. (b) Fernández, M. C.; Quintela, J. M.; Ruiz, M.; Ojea, V. *Tetrahedron: Asymmetry* **2002**, *13*, 233−237. (c) Fernández, M. C.; Ruiz, M.; Ojea, V.; Quintela, J. M. *Tetrahedron Lett.* **2002**, *43*, 5909−5912.

SCHEME 1

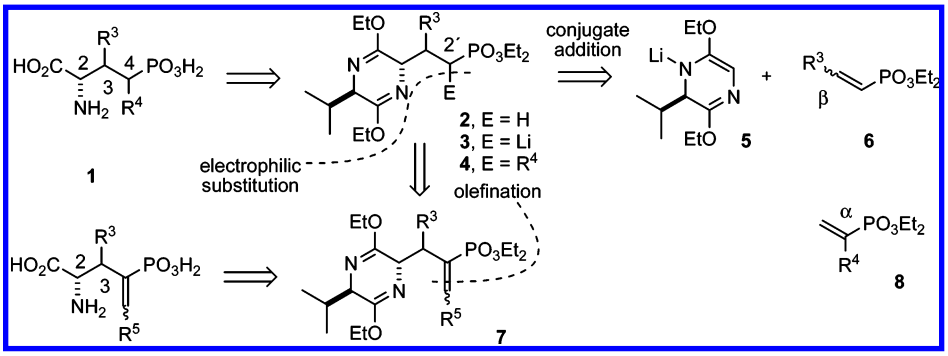

CHART 2

Structure	Numeral	Stereochemistry
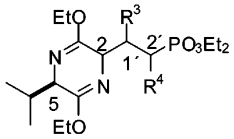	**11**	2,5-trans
	12	2,5-trans-2,2′-syn
	13	2,5-trans-2,2′-anti
	14	2,5-cis-2,2′-anti
	15	2,5-cis-2,2′-syn
	17	2,5-trans-2,1′-syn
	18	2,5-trans-2,1′-anti
	19	2,5-trans-2,1′-syn-1′,2′-syn
	20	2,5-trans-2,1′-syn-1′,2′-anti
	21	2,5-trans-2,1′-anti-1′,2′-anti
	22	2,5-trans-2,1′-anti-1′,2′-syn
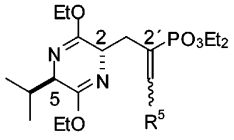	**23**	2,5-trans-2′-*Z*
	24	2,5-trans-2′-*E*
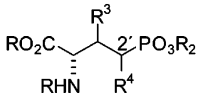	**27**,**28**,**29**	2,4-syn
	31,**32**,**33**	2,4-anti
	35,**36**	2,3-syn-3,4-syn
	37,**38**	2,3-syn-3,4-anti
	39,**40**	2,3-anti-3,4-anti
	41,**42**	2,3-anti-3,4-syn
	43	2,4-syn
	47	2,4-anti
	51	2,3-syn-3,4-anti
	54	2,3-anti-3,4-syn
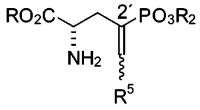	**27**,**28**	2′-*Z*
	31,**32**	2′-*E*
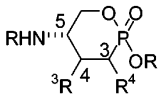	**45**,**46**	3,5-cis
	49,**50**	3,5-trans
	52,**53**	3,4-cis-4,5-trans
	55	3,4-trans-4,5-cis

Legend	R^3	R^4	R^5
aa	H	H	–
ab	H	Me	–
ac	H	CHO	–
ad	H	CO_2Et	–
ae	H	F	–
af	H	OH	–
ag	H	PO_3Et_2	–
ag*	H	PO_3H_2	–
ah	H	$SnPh_3$	–
ai	H	$SiMe_3$	–
aj	H	N_3	–
ak	H	Bn	–
am	H	–	Ph
an	H	–	*i*-Pr
ao	H	–	2-C_4H_3S
ap	H	–	CHCHPh
aq	H	$-(CH_2)_5-$	
ar	H	NH_2	–
ma	Ph	H	–
mb	Ph	Me	–
na	*i*-Pr	H	–
nb	*i*-Pr	Me	–

phonate **10** is much faster than the reaction with **9**. The initially formed phosphonate carbanion then is trapped by **9** in a dehydrohalogenation reaction regenerating the acceptor **10**.

Slow addition of the bis-lactim ether **11aa** to a solution of LDA in THF at −78 °C was followed 15 min later by the dropwise addition of the electrophilic reagent. Reactions with methyl iodide (MeI), trimethylsilyl chloride (TMSCl), *N*-fluorobenzenesulfonimide (NFSi),[16] Ph_3SnCl, Et_2CO_3, Et_2PO_3-Cl, triisopropylbenzenesulfonyl azide (trisyl-N_3),[17] DMF, or HCO_2Et took place rapidly at −78 °C. When necessary, processes were quenched 5 min later by the addition of a proton source. As the reaction with MoO_5·Py·HMPA (MoOPH)[18]

SCHEME 2

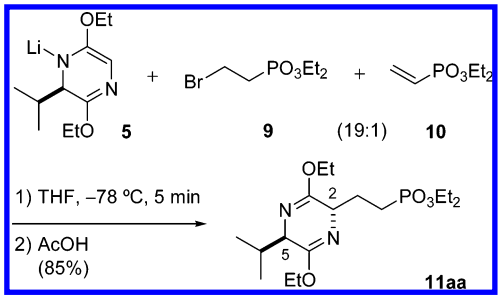

(15) Addition of **9** to the lithium salt **5** under the described conditions[9b] gave a mixture of **11aa** and its 2,5-cis epimer in ca. 85:15 ratio. For previous alkylations of lithiated bis-lactim ether with low diastereoselectivity, see: (a) Ma, C.; Liu, X.; Li, X.; Flippen-Anderson, J.; Yu, S.; Cook, J. M. *J. Org. Chem.* **2001**, *66*, 4525−4542. (b) Adamczyk, M.; Akireddy, S. R.; Reddy, R. E. *Tetrahedron: Asymmetry* **1999**, *10*, 3107−3110. (c) Bull, S. D.; Chernega, A. N.; Davies, S. G.; Moss, W. O.; Parkin, R. M. *Tetrahedron* **1998**, *54*, 10379−10388.

(16) Differding, E.; Duthaler, R. O.; Krieger, A.; Rüegg, G. M.; Schmit, C. *Synlett* **1991**, 395−397.

(17) Evans, D. A.; Britton, T. C.; Ellman, J. A.; Dorow, R. L. *J. Am. Chem. Soc.* **1990**, *112*, 4011−4030.

SCHEME 3[a]

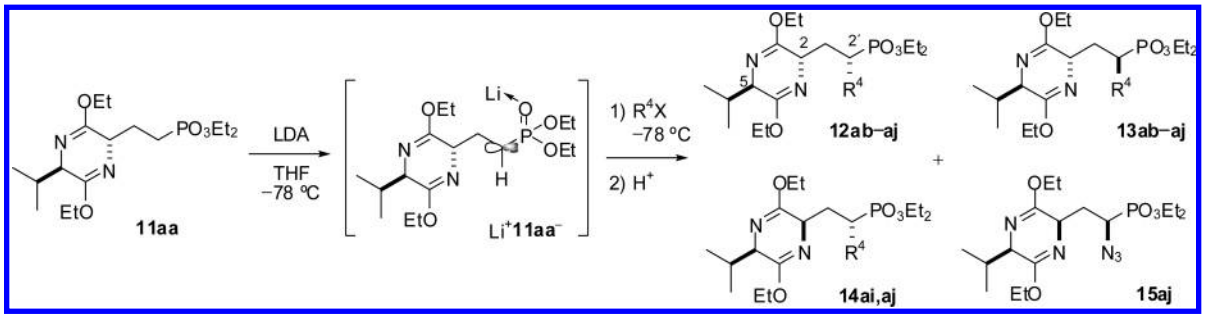

[a] Legend: **b**, R^4 = Me; **c**, R^4 = CHO; **d**, R^4 = CO_2Et; **e**, R^4 = F; **f**, R^4 = OH; **g**, R^4 = PO_3Et_2; **h**, R^4 = $SnPh_3$; **i**, R^4 = $SiMe_3$; **j**, R^4 = N_3.

TABLE 1. Electrophilic Substitutions on Li^+11aa$^-$

legend	electrophile	H^+ source	yield (%)[a]	**12**:**13**:**14**:**15** ratio[b]
b	MeI		84	3:2:−:−
c	HCO_2Et	HOAc	75	1:1:−:−
d	Et_2CO_3	HOAc	66	2:1:−:−
e	NFSi		66	3:1:−:−
f	MoOPH	H_2O	59	2:1:−:−
g	Et_2PO_3Cl	HOAc	83	*c*
h	Ph_3SnCl		75	3:2:−:−
i	Me_3SiCl		85	4:1:1:−
j	Trisyl-N_3	HOAc/KOAc	80	7:7:1:1
k	BnBr		NR	
l	DEAD		NR	

[a] Isolated yield of mixtures of adducts, after column chromatography. [b] Determined by integration of the ^{31}P NMR spectra of the crude mixtures. [c] There is not anti/syn isomerism in this case. No reaction (NR) was observed upon warming up to 0 °C.

proceeded slowly at −78 °C, it was allowed to reach −10 °C and was quenched with water after 4 h. Conversely, no reaction was observed under these conditions or with longer reaction times and warming (up to 10 h and 0 °C) with either benzyl bromide or DEAD.

After workup, the ^{31}P NMR analysis of the crude mixtures revealed a highly regioselective course for the substitution process, which led to the exclusive formation of mixtures of 2′-substituted bis-lactims **12**−**15ab**−**aj** despite the literature[9b,19] (see Scheme 3). Integration of the ^{1}H decoupled ^{31}P NMR spectra also revealed moderate levels of asymmetric induction at the substitution position, which depended on the nature of the electrophilic reagent (see Table 1). In this way, methylation, formylation, carboxylation, fluorination, hydroxylation, phosphorylation, and stannylation of **11aa** took place with a complete retention of the 2,5-trans configuration of the bis-lactim ether and afforded mixtures of the 2,2′-anti and 2,2′-syn substituted products **12ab**−**ah** and **13ab**−**ah,** respectively, with ratios ranging from 1:1 to 3:1. In contrast, the silylation and the azidation, which were regioselective at the 2′-position, took place with a significant degree of racemization at position 2 and led to mixtures of the 2,5-cis and 2,5-trans diastereoisomers. Thus, the silylation led to a mixture of bis-lactims **12ai/13ai/14ai** in a 4:1:1 ratio, while the azides **12aj/13aj/14aj/15aj** were obtained in a 7:7:1:1 ratio.

After flash chromatography of the crude mixture, the fractions containing the 2′-substituted bis-lactims were isolated in 59−85% combined yield along with 5−15% of unreacted starting material. Electrophilic fluorination with NFSi also afforded 2,5-trans-2′,2′-difluorinated bis-lactim **16ae** in 10% yield (see Scheme 4). The use of 2 equiv of NFSi resulted in the complete reaction of **11aa** and a reduced ratio of mono- to difluorination (4:3 instead of 11:1) with neither change in the combined yield (72%) nor the level of 2,2′-syn stereoselectivity. When LDA was added to the preformed equimolar mixture of **11aa** and NFSi, a 65% conversion to the monofluorinated products **12ae/13ae** was achieved. As the difluorination was completely suppressed in this case, the yield of **12ae/13ae** could be increased to 78% by resubjecting the recovery material to these fluorination conditions.

SCHEME 4

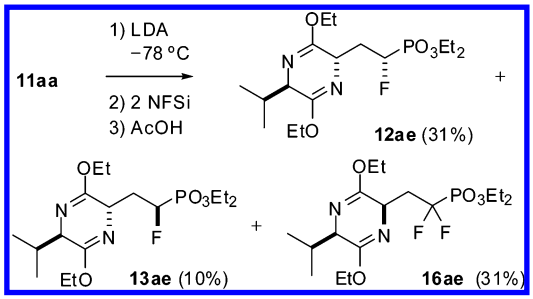

Having shown the feasibility of performing electrophilic substitutions on lithiated bis-lactim ether **11aa**, we explored the extension of this reactivity to 1′-substituted bis-lactim ethers derived from *cyclo*-[L-AP4-D-Val] using the methylation as the model process. To determine the influence of the nature and configuration of the substituent on the facial selectivity of the methylation, bis-lactim ethers with phenyl- or isopropyl- groups at the 1′-position and 2,1′-syn or 2,1′-anti configurations were stereoselectively prepared. Following our recently reported procedure,[12a] the conjugate additions of lithium salt **5** to *β*-phenyl- and *β*-isopropyl-substituted vinylphosphonates of (*Z*)-configuration afforded bis-lactim ethers **17ma** and **17na** with 2,5-trans-2,1′-syn configuration, while additions to the corresponding (*E*)-vinylphosphonates gave rise to 2,5-trans-2,1′-anti bis-lactims **18ma** and **18na** (see Scheme 5).

Phosphonate carbanions Li^+**17ma**$^-$, Li^+**17na**$^-$, Li^+**18ma**$^-$, and Li^+**18na**$^-$ were generated by the addition of the corresponding bis-lactim ethers to solutions of LDA at −78 °C in THF. When methyl iodide was added to the phosphonate carbanions as above, reactions also took place in a highly regioselective fashion with complete retention of the configuration at positions 2, 5, and 1′ and afforded mixtures of the corresponding 2′-methylated bis-lactims in very good yields. According to the ^{31}P NMR analysis of the crude mixtures, the methylation of 2,1′-syn phosphonate carbanions Li^+**17ma**$^-$ and

(18) Vedejs, E.; Larsen, S. *Org. Synth.* **1986**, *64*, 127−137, and references therein.

(19) Vassiliou, S.; Dimitropoulus, C.; Magriotis, P. A. *Synlett* **2003**, 2398−2400.

SCHEME 5[a]

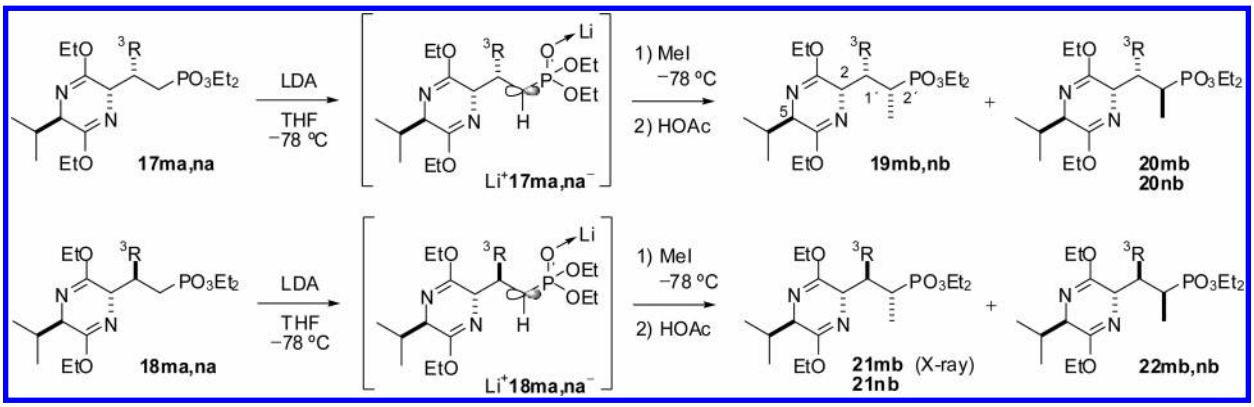

[a] Legend: **m**, R^3 = Ph; **n**, R^3 = *i*-Pr.

SCHEME 6[a]

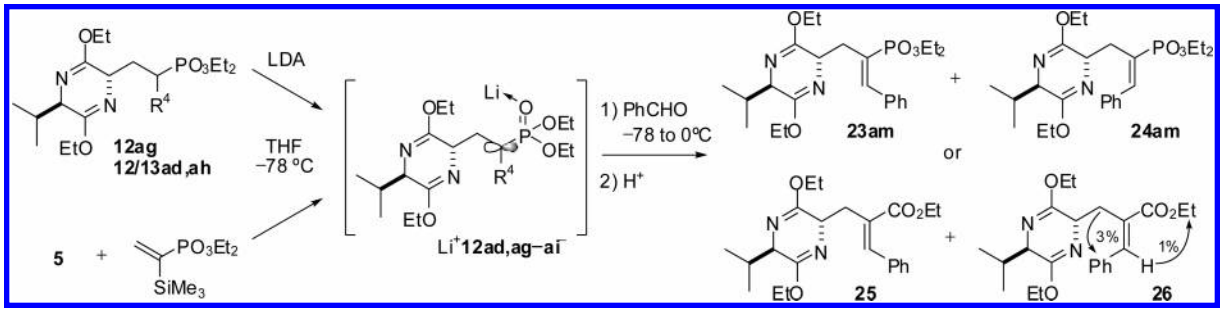

[a] Legend: **d**, R^4 = CO_2Et; **g**, R^4 = PO_3Et_2; **h**, R^4 = $SnPh_3$; **i**, R^4 = $SiMe_3$.

Li^+**17na**$^-$ was found 1′,2′-anti stereoselective and furnished mixtures of bis-lactims **19**/**20mb** and **19**/**20nb** with 1:3 and 1:6 ratios, respectively. Conversely, the reaction of the phosphonate carbanions with 2,1′-anti configuration was not regular: methylation of Li^+**18ma**$^-$ also was found 1′,2′-anti stereoselective and gave a 3:1 mixture of bis-lactims **21mb** and **22mb**, while the reaction of Li^+**18na**$^-$ was 1′,2′-syn selective and afforded **21nb** and **22nb** with 1:3 ratio. Upon crystallization from hexanes, bis-lactim ether **21mb** yielded crystals amenable to X-ray structure determination, which allowed the confirmation of its relative stereochemistry (see Supporting Information).

Olefination of Carbonyl Compounds with Bis-lactim Ethers Derived from *cyclo*-[L-AP4-D-Val]. To explore further the scope of these electrophilic substitutions, we examined the olefination reactions of carbonyl compounds using the α-ethoxycarbonyl-, α-trimethylsilyl-, α-diethoxyphosphoryl-, and α-triphenylstannyl-stabilized phosphonate carbanions derived from bis-lactim ethers **12**/**13ad**,**ag**−**ai**. Toward this end, Li^+**12ad**$^-$, Li^+**12ag**$^-$, and Li^+**12ah**$^-$ were prepared by adding **12ag** or mixtures of **12**/**13ad**,**ah** to solutions of LDA at −78 °C in THF, while phosphonate carbanion Li^+**12ai**$^-$ was obtained free of its 2,5-cis diastereoisomer by adding α-trimethylsilylvinylphosphonate to a solution of lithium azaenolate **5**[12a] (see Scheme 6). Benzaldehyde, which was selected as a model carbonyl compound, was slowly added 15 min later, and the reaction mixtures were gradually warmed to 0 °C during 4 h. After the reaction mixtures were subjected to quenching with acetic acid and aqueous workup, the 2′-benzylidene substituted 2,5-trans bis-lactims ethers **23am**/**24am** and **25**/**26** were isolated in 56−77% yield, along with 10−25% of unreacted starting materials. Because the unreacted bis-lactim ethers **12**/**13ad**,**ag**,**ah** could almost completely be recovered and showed no racemization, the yield of these olefinations could be increased to 70−85% by resubjecting the recovered material to the same reaction conditions.

Analysis of the ^1H and ^{31}P NMR spectra of the crude mixtures revealed different stereochemical courses and selectivities in the Wadsworth−Emmons olefinations. Thus, α-ethoxycarbonyl-stabilized phosphonate carbanion Li^+**12ad**$^-$ led to a 1:6 mixture of cinnamates **25** and **26** with 2,5-trans-(2′*Z*) and 2,5-trans-(2′*E*) configurations, respectively,[20] while olefination with the α-diethoxyphosphoryl-substituted phosphonate carbanion Li^+**12ag**$^-$ took place with (*Z*)-stereoselection and afforded vinylphosphonates **23am** and **24am** in a 5:1 ratio. This result is remarkable, because lithioalkylidenebisphosphonates have been reported to selectively produce *β*- and α,*β*-substituted vinylphosphonates with (*E*)-configuration in their reactions with carbonyl compounds.[21] Peterson olefinations of phosphonate carbanions Li^+**12ah**$^-$ and Li^+**12ai**$^-$ showed markedly different levels of (*Z*)-stereoselection. In this way, the α-trimethylsilyl-stabilized phosphonate carbanion led to vinylphosphonates **23am** and **24am** in a 3:2 ratio. When starting with the α-triphenylstannyl substituted bis-lactims **12**/**13ah**, the olefination gave rise exclusively to the (*Z*)-vinylphosphonate **23am**. The stereochem-

(20) Stereochemical assignments for the cinnamate derivatives **25** and **26** were consistent with the sets of observed NOEs (see Scheme 6).

(21) (a) Gupta, A.; Sacks, K.; Khan, S.; Tropp, B. E.; Engel, R. *Synth. Commun.* **1980**, *10*, 299−304. (b) Aboujaoude, E. E.; Lietjé, S.; Collignon, N.; Teulade, M. P.; Savignac, P. *Tetrahedron Lett.* **1985**, *26*, 4435−4438. (c) Teulade, M. P.; Savignac, P.; Aboujaoude, E. E.; Liétge, S.; Collignon, N. *J. Organomet. Chem.* **1986**, *304*, 283−300. (d) Kiddle, J. J.; Babler, J. H. *J. Org. Chem.* **1993**, *58*, 3572−3574. (e) Perlikowska, W.; Mphahlele, M. J.; Modro, T. A. *J. Chem. Soc., Perkin Trans. 2* **1997**, 967−970. (f) Iorga, B.; Eymery, F.; Savignac, P. *Tetrahedron Lett.* **1998**, *39*, 4477−4480. (g) Chang, K.; Ku, B.; Oh, D. Y. *Synth. Commun.* **1989**, *19*, 1891−1898.

SCHEME 7[a]

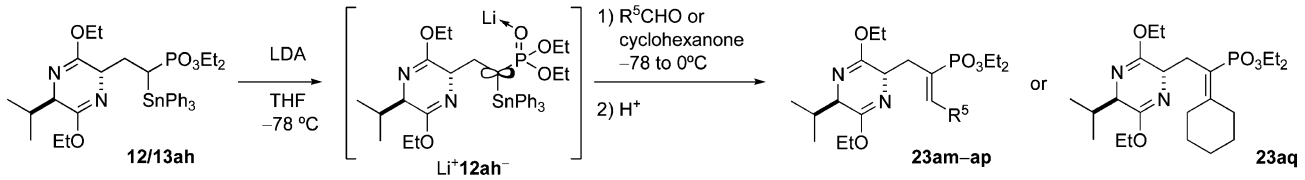

[a] Legend: **m**, R^5 = Ph; **n**, R^5 = *i*-Pr; **o**, R^5 = 2-C_4H_3S; **p**, R^5 = CHCHPh.

ical course of the tin−Peterson olefination with Li^+**12ah**$^-$ is similar to that previously encountered in the preparation of other α,*β*-substituted vinylphosphonates.[22]

Prompted by the excellent stereoselectivity achieved in the benzylidenation of the α-triphenylstannyl-stabilized phosphonate carbanion Li^+**12ah**$^-$, we prepared a series of vinylphosphonates **23am−aq** in moderate yield by application of these tin−Peterson reactions to various structurally diverse carbonyl compounds (see Scheme 7). Thus, solutions of isobutyraldehyde, 2-thienylcarboxaldehyde, cinnamaldehyde, or cyclohexanone in THF were added dropwise to solutions of Li^+**12ah**$^-$ in THF at −78 °C, and the reaction mixtures were gradually warmed to 0 °C during 4 h. After the reaction mixtures were subjected to quenching with acetic acid and aqueous workup, vinylphosphonates **23an−aq** were isolated in 50−61% yield along with 10−32% of unreacted starting materials. After inspection of the ^{31}P NMR spectra of the crude mixtures, we could not detect any absorption corresponding to the minor (*E*)-isomers, as was previously encountered in the reaction of Li^+**12ah**$^-$ with benzaldehyde. Thus, the tin−Peterson olefinations of either α-branched, α,*β*-unsaturated, aromatic, or heteroaromatic aldehydes using the α-triphenylstannylphosphonate lithium salt derived from *cyclo*-[L-AP4-D-Val] took place with an outstanding level of stereoselection giving rise exclusively to the kinetically favored (*Z*)-vinylphosphonates.

Finally, catalytic hydrogenation of the vinylphosphonates **23am** or **24am** afforded a 1:2 mixture of 2,2′-syn and 2,2′-anti 2′-benzylated bis-lactim ethers, **12ak** and **13ak**, respectively, which could not be prepared by treatment of Li^+**11aa**$^-$ with benzyl bromide.

Computational Studies. Stereochemical Model for the Electrophilic Substitution on Bis-lactim Ethers Derived from *cyclo*-[L-AP4-D-Val]. The origin of *π*-facial stereoselectivity of enolates and related carbanions remains a controversial area of investigation.[23] A combination of torsional strain, stereoelectronic effects, steric factors, and chelation may be operative in defining the stereochemical outcome for the electrophilic substitutions on lithium phosphonate carbanion Li^+**11aa**$^-$. In this manner, the observed 2,2′-syn selectivity can be rationalized by considering the involvement of seven- or eight-membered intermediate chelate complexes such as **i7** or **i8**, which should react with the electrophile by its less hindered face (See Scheme 8).

To gain more insight into the stereocontrol elements determining the selectivity of these substitutions, we have performed a computational study of the conformational space accessible

SCHEME 8

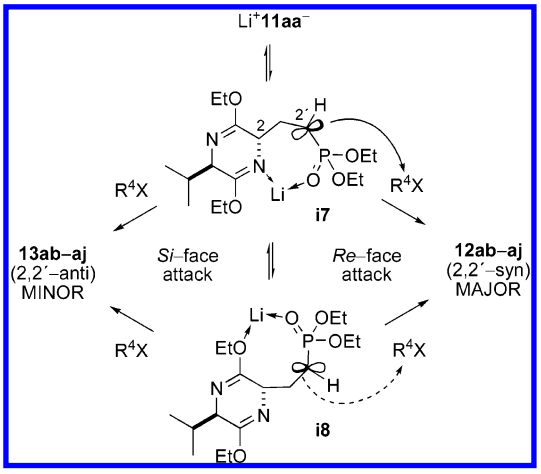

to the phosphonate carbanion Li^+**11aa**$^-$ and of its possible reaction pathways with two model electrophiles: methyl iodide and trimethylsilyl chloride. Because low reagent concentration will promote the reaction via the more highly solvated and less aggregated species,[24] complete dissociation of the possible oligomeric clusters was assumed by considering discrete solvation of the lithium with two THF molecules.[25] The geometry optimizations were performed using a B3LYP density functional theory (DFT) procedure[26] with the cc-pVDZ basis set[27] and a small-core relativistic pseudopotential (PP) for I.[28] Single point energy calculations of the bulk solvent effect also were performed in THF (ϵ = 7.52) using Tomasi's PCM method[29] at the B3LYP/cc-pVTZ-PP level[27] (see Computational Methods in Supporting Information).

Conformer search for the seven- and the eight-membered chelate complexes of disolvated Li^+**11aa**$^-$ gave four different families of structures. These sets were characterized by either a "compact" or an "extended" disposition of the phosphonate and bis-lactim ether moieties due to synclinal or anticlinal N(1)C(2)C(1′)C(2′) dihedrals, respectively. Most stable members of each family display a nearly planar sp^2 carbanionic carbon

(22) Mimouni, N.; About-Jaudet, E.; Collignon, N.; Savignac, P. *Synth. Commun.* **1991**, *21*, 2341−2348.

(23) (a) Soteras, I.; Lozano, O.; Gómez-Esqué, A.; Escolano, C.; Orozco, M.; Amat, M.; Bosch, J.; Luque, F. J. *J. Am. Chem. Soc.* **2006**, *128*, 6581−6588. (b) Ando, K. *J. Am. Chem. Soc.* **2005**, *127*, 3964−3972. (c) Ikuta, Y.; Tomoda, S. *Org. Lett.* **2004**, *6*, 189−192. (d) Ando, A.; Green, N. S.; Li, Y.; Houk, K. N. *J. Am. Chem. Soc.* **1999**, *121*, 5334−5335.

(24) Abbotto, A.; Streitwieser, A.; Schleyer, P. v. R. *J. Am. Chem. Soc.* **1997**, *119*, 11255−11268. (b) Abbotto, A.; Leung, S. S.-W.; Streitwieser, A. *J. Am. Chem. Soc.* **1998**, *120*, 10807−10813.

(25) The microsolvation approach has been successfully used for the theoretical study of numerous other solvated lithium compounds, see: Mogali, S.; Daville, K.; Pratt, L. M. *J. Org. Chem.* **2001**, *66*, 2368−2373 and references therein.

(26) (a) Becke, A. D. *J. Chem. Phys.* **1993**, *98*, 5648−5652. (b) Lee, C.; Yang, W.; Parr, R. G. *Phys. Rev. B* **1988**, *37*, 785−789.

(27) (a) Davidson, E. R. *Chem. Phys. Lett.* **1996**, *260*, 514−518. (b) Woon, D. E.; Dunning, T. H., Jr. *J. Chem. Phys.* **1993**, *98*, 1358−1371. (c) Dunning, T. H., Jr. *J. Chem. Phys.* **1989**, *90*, 1007−1023.

(28) Peterson, K. A.; Figgen, D.; Goll, E.; Stoll, H.; Dolg, M. *J. Chem. Phys.* **2003**, *119*, 11113−11123.

(29) (a) Cossi, M.; Scalmani, G.; Rega, N.; Barone, V. *J. Chem. Phys.* **2002**, *117*, 43−54. (b) Mennucci, B.; Tomasi, J. *J. Chem. Phys.* **1997**, *106*, 5151−5158.

SCHEME 9

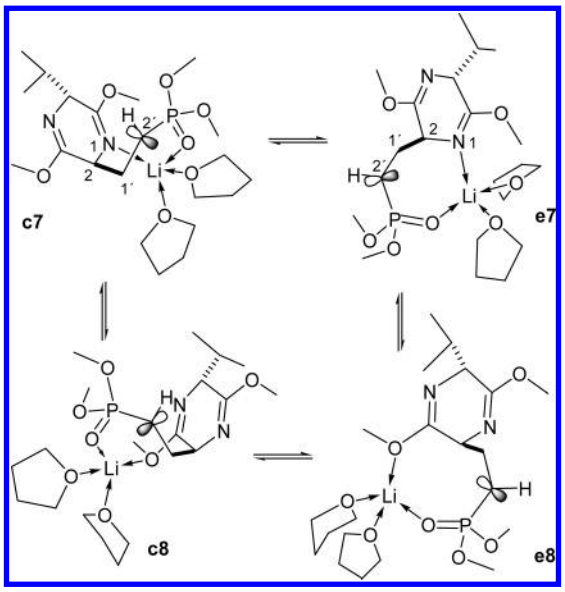

TABLE 2. Relative Energies, Dipole Moments, and Populations Calculated for Models of Disolvated Li$^+$11aa$^-$

	gas phase			THF	
model	rel E^a (kcal/mol)	population (%)^b	μ^c (D)	rel E^d (kcal/mol)	population (%)^b
c7	2.0	0.35	8.4	0.0	100
e7	0.2	37.96	5.0	4.3	0
c8	2.9	0.04	7.7	3.3	0
e8	0.0	61.65	6.0	4.0	0

[a] Calculated at B3LYP/cc-pVTZ-PP//B3LYP/cc-pVDZ-PP level. [b] Relative abundance calculated at 195.15 K (−78 °C). [c] Calculated dipole moment in debyes. [d] Calculated at B3LYP/cc-pVTZ-PP//B3LYP/cc-pVDZ-PP level using the PCM method.

(sum of the angles at the carbons = 358−360°) and a synperiplanar C(1′)C(2′)P(OLi) dihedral, which allows an effective hyperconjugative stabilization by carbanionic lone-pair overlap with an appropriate σ^*(P−O) orbital. In the gas phase, the two most stable extended intermediates (**e7** and **e8**, see Scheme 9) were calculated to be more than 1.8 kcal/mol lower in energy than the most stable compact ones (**c7** and **c8**). Because of their higher dipole moments, the compact chelate complexes were more susceptible to the electrostatic field of the solvent and were found to be more stable than the extended conformers in the polarizable continuum. In particular in THF solution, the most stable compact seven-membered chelate complex **c7** was calculated to be more than 3.3 kcal/mol lower in energy than the rest of the intermediates (see Table 2 and Supporting Information, Figure S2).

While the extended chelate complexes **e7** and **e8** have both faces of the carbanionic carbon accessible to the electrophile, the *Si*-face of **c7** and the *Re*-face of **c8** appear effectively shielded by the bis-lactim ether. Thus, a combination of steric factors, chelation, and solvent effects may determine the stereoselectivity of the electrophilic substitution. In solution, the major syn product may be derived from the most stable seven-membered chelate intermediate (**c7**) by reaction through its less hindered face, while the formation of the secondary anti product could require the approach of the electrophile to the more crowded face of **c7**, or the intervention of a less-stabilized eight-membered chelate complex like **c8**. To test this hypothesis, the reaction pathways for both 2,2′-anti and 2,2′-syn attack of electrophiles on the four different chelate complexes were analyzed next. The approach of methyl iodide to the *Re*-face of the carbanionic carbon at the chelate intermediates led to the location of four 2,2′-syn transition structures that were designated as **c7s**, **e7s**, **c8s**, and **e8s**, respectively. The corresponding methylations through the *Si*-faces of the chelate complexes gave rise to four transition structures in the 2,2′-anti reaction pathway that were designated as **c7a**, **e7a**, **c8a**, and **e8a**. In an analogous fashion, eight different transition structures (from **c7s** to **e8a**) were located for the reaction of the intermediate chelate complexes with trimethylsilyl chloride.

In the gas phase, the most favorable transition structure for the methylation was **e7s**, which was derived from the extended seven-membered chelate complex **e7** (see Figure 1). This syn transition structure was favored 1.9 kcal/mol over the corresponding most favorable anti transition structure **e8a**, which also showed an extended conformation derived from the eight-membered intermediate **e8** (see Table 3). The syn transition structure **e7s** showed a staggered arrangement of all the vicinal bonds at the carbanionic carbon undergoing the hybridization change and no visible steric interactions, while the anti transition structure **e8a** occurred with a rather eclipsed arrangement (C(2)C(1′)C(2′)CH_3 dihedral angle is 26°) and exhibited a repulsive interaction between a hydrogen of the incoming electrophile and one nitrogen of the bis-lactim ring. The distance between these two atoms was 2.40 Å, which was shorter than the sum of their van der Waals radii (2.75 Å).

Methylation through **e7s** and **e8a**, which are the major transition structures in the gas phase, almost vanished in THF solution. Instead, two transition structures (**c7s** and **c8a**) that do not proceed in the gas phase and are characterized by compact conformations of higher dipole moment became the most important structures in solution. Both transition structures showed an almost perfect staggered arrangement of all the vicinal bonds at the carbanionic carbon (C(2)C(1′)C(2′)CH_3 dihedral angle higher than 176°) and no visible steric interactions with the incoming electrophile. In THF solution, the syn transition structure **c7s** was calculated to be 1.4 kcal/mol more favorable than the anti transition structure **c8a**. Other competitive transition structures showed repulsive interactions with the electrophile (**c7a** and **c8s**), torsional strain (all four), or loss of hyperconjugative stabilization (**c7a** and **e8s**) due to nearly eclipsed arrangements at the carbanionic carbon, and these transition structures were found to be higher in energy (see Supporting Information, Figure S3).

For the silylation process, the transition structures **e8s** and **e7a** were calculated as the most stable in the gas phase (see Table 3). As previously found for the methylation process, the extended transition structures vanished in THF, and the compact transition structures **c7s** and **c8a**, which have higher dipole moments, became the most favorable syn and anti transition structures, respectively. These transition structures lay in different positions along the reaction coordinate, with C−Si bond lengths of 2.5 and 2.9 Å for **c7s** and **c8a**, respectively (see Figure 2). In addition, the syn transition structure **c7s** showed a nearly staggered arrangement at the carbanionic carbon (C(2)C(1′)C(2′)Si dihedral angle of 155°), while the anti transition structure **c8a** occurred with an eclipsed arrangement. In agreement with the experimental trend, the syn transition structure **c7s** was found to be 4.9 kcal/mol lower in energy than the anti transition structure **c8a** in the THF solution (see Table 3).

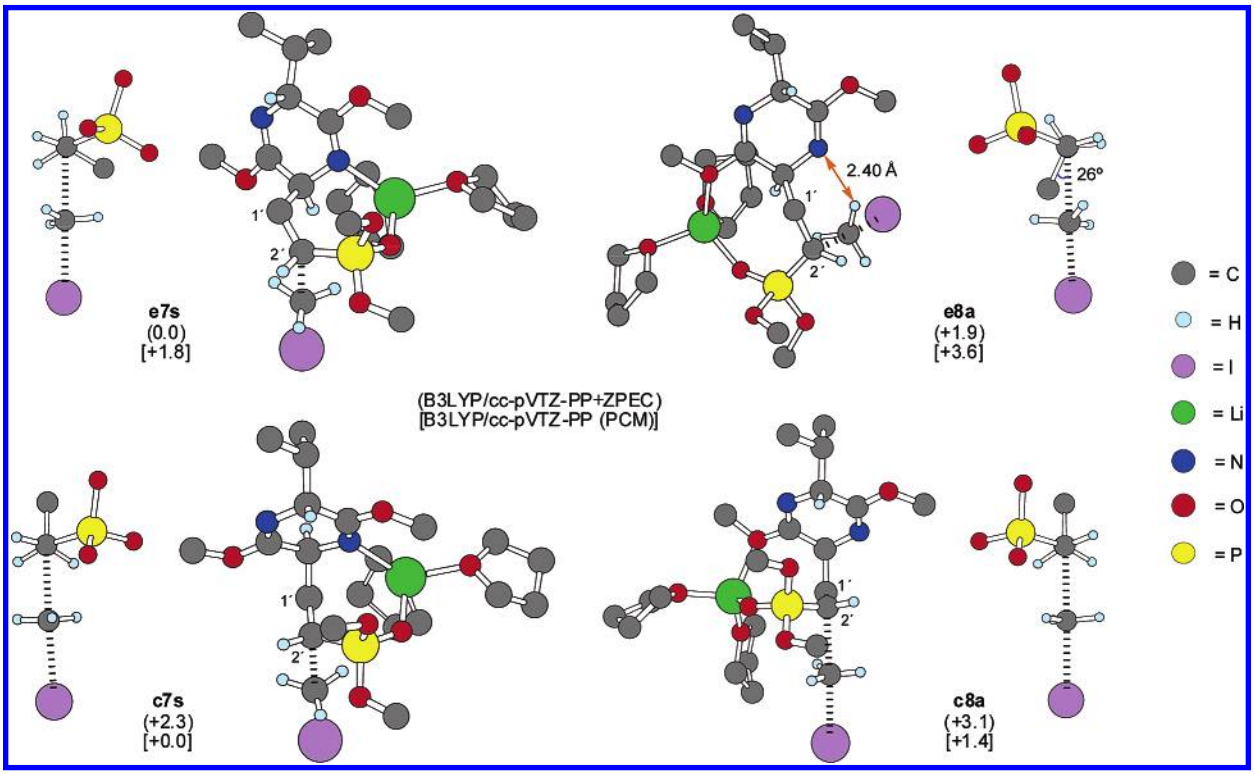

FIGURE 1. Chem3D representations for the most favored transition structures located (at B3LYP/cc-pVDZ-PP level) for the anti and syn attacks of MeI on Li^+**11aa**$^-$. Relative energies in the gas phase (at B3LYP/cc-pVTZ-PP+ZPVEC level) and in THF (at B3LYP/cc-pVTZ-PP (PCM) level) are shown in parentheses and brackets, respectively (kcal/mol). Newman projections are views along C(2′)C(1′) bonds. The hydrogen atoms are omitted for clarity except at chiral and reaction centers.

TABLE 3. Relative Energies and Dipole Moments Calculated for Transition Structures

	methylation			silylation		
	THF		vacuo	THF		vacuo
model	rel $E^{a,b}$	μ^c	E rel[a]	rel $E^{d,b}$	μ^c	rel E^d
c7s	0.0	15.9	2.3	0.0	19.4	3.0
e7s	1.8	14.3	0.0	6.3	15.6	2.4
c8s	5.3	14.4	4.9	15.1	15.3	12.4
e8s	4.3	19.7	2.9	6.8	17.2	0.0
c7a	7.1	16.9	6.4	10.9	17.0	9.4
e7a	3.6	14.3	2.1	7.8	16.4	1.3
c8a	1.4	14.5	3.1	4.9	17.0	1.4
e8a	6.4	13.1	1.9	7.5	15.5	6.4

[a] Calculated at B3LYP/cc-pVTZ-PP//B3LYP/cc-pVDZ-PP level, in kcal/mol. [b] Calculated using the PCM method in kcal/mol. [c] Dipole moment in debyes. [d] Calculated at B3LYP/cc-pVTZ//B3LYP/cc-pVDZ level in kcal/mol.

In summary, the computational models reproduced the sense and degree of stereoselection in the reactions of phosphonate carbanion Li^+**11aa**$^-$ with methyl iodide and trimethylsilyl chloride: syn transition structures are favored over the anti counterparts in both processes, and the energy difference between the competitive transition structures was greater for the silylation than for the methylation. Nevertheless, the calculated syn/anti ratios (assuming a Boltzmann distribution of the transition structures at −78 °C) were considerably higher than the experimental values. The modeling studies provided some valuable insight to rationalize the stereochemical results of the substitutions. Calculations suggested that the syn selectivity in the electrophilic substitutions of Li^+**11aa**$^-$ may have originated from the intervention of seven- and eight-membered chelate structures. In THF solution, these intermediates preferentially adopted compact conformations (with higher dipole moments) in which the bis-lactim ether moiety effectively shielded one of the faces of the carbanionic carbon and furnished facial bias in the electrophilic substitution process. The higher syn selectivity observed in the silylation process can be understood as a consequence of an increased torsional strain in the anti transition structures because of the higher steric requirements of the trimethylsilyl group.

Stereochemical Model for the Olefination of Bis-lactim Ethers Derived from *cyclo*-[L-AP4-D-Val]. We have shown that tin−Peterson olefinations of aldehydes **27m**−**p** using the α-triphenylstannyl-stabilized phosphonate carbanion Li^+**12ah**$^-$ take place with complete (*Z*)-selectivity and give rise to vinylphosphonates **23am**−**ap** (See Scheme 7). To identify the selectivity-determining step and localize the factors that influence the stereochemical outcome of the process, we have studied the tin−Peterson benzylidenation of Li^+**12ah**$^-$ by using computational methods.

Although Peterson olefinations with stabilized anions afford stereoselectivities comparable to those obtained with Wittig-type reactions, experimental and theoretical efforts devoted to elucidate its mechanistic details have been scattered.[30] It is generally accepted that Peterson olefination involves formation and cleavage of a four-membered intermediate. When carbanions are stabilized by functional groups capable of chelation control, stepwise mechanisms seem to be favored over the concerted ones in both the formation and the cleavage steps. By analogy with previous theoretical studies on the closely

(30) (a) van Staden, L. F.; Gravestock, D.; Ager, D. J. *Chem. Soc. Rev.* **2002**, *31*, 195−200. (b) Kano, N.; Kawashima, T. The Peterson and related reactions. In *Modern Carbonyl Olefination;* Takeda, T., Ed; Wiley-VCH: Weinheim, Germany, 2004; pp 18−103.

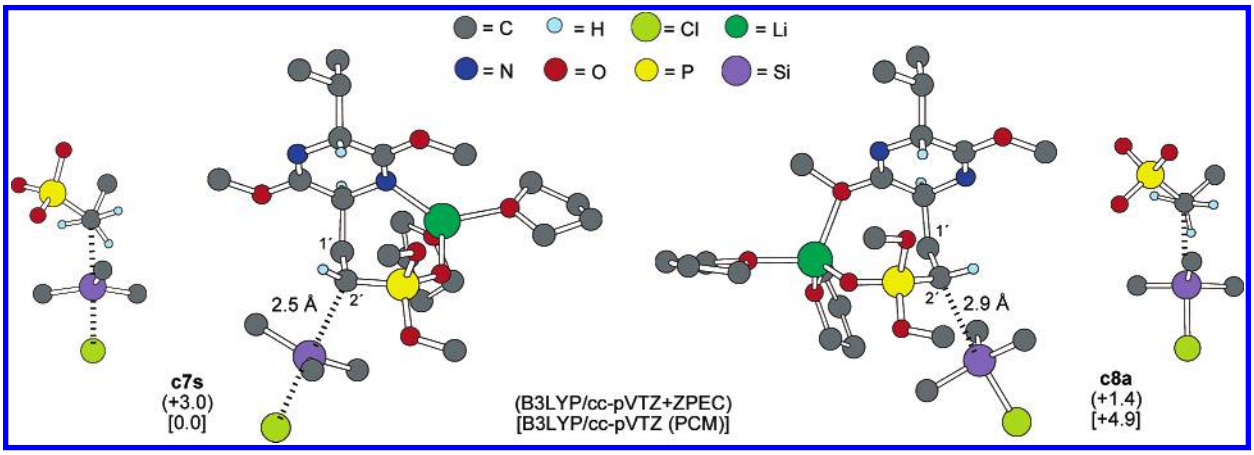

FIGURE 2. Chem3D representations for the most favored transition structures located (at B3LYP/cc-pVDZ level) for the anti and syn attacks of TMSCl on Li^{+}**11aa**$^{-}$. Relative energies in the gas phase (at B3LYP/cc-pVTZ+ZPEC level) and in THF (at B3LYP/cc-pVTZ (PCM) level) are shown in parentheses and brackets, respectively (kcal/mol). Newman projections are views along C(2′)C(1′) bonds. The hydrogen atoms are omitted for clarity except at chiral and reaction centers.

SCHEME 10

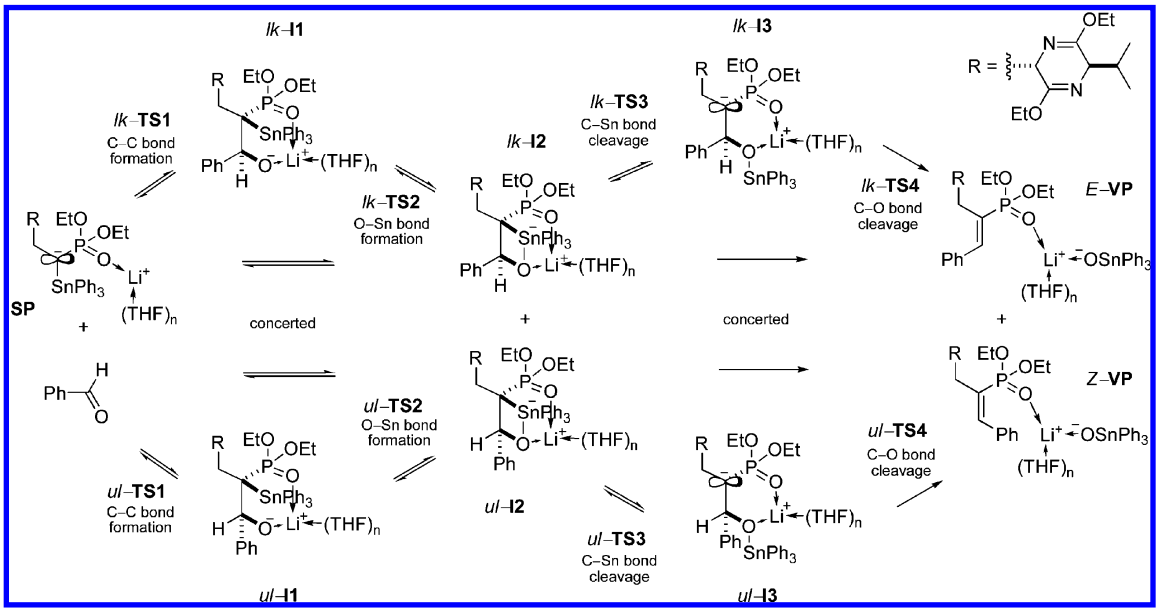

related Peterson olefinations with the α-silyl ester enolates,[31] the stepwise pathway for the reaction between the α-stannyl-stabilized phosphonate carbanion (SP, see Scheme 10) and benzaldehyde should involve an initial phosphonate carbanion addition to the carbonyl group (C−C bond formation) to form a lithium-coordinated oxyanion intermediate (**I1**) and be followed by an O−Sn bond formation to afford a 1,2-oxastannetanide intermediate (**I2**). Subsequently, cleavage of the C−Sn bond to give a new phosphonate-stabilized carbanion (**I3**) would be followed by lithium stannoxide elimination (C−O bond cleavage) to yield the vinylphosphonates (VP). If the elimination step is fast and phosphonate carbanions **I3** are not long-lived enough for C−C bond rotation, crossover between the diastereomeric pathways should not take place. According to this hypothesis, the selective formation of (*Z*)-vinylphosphonate, (*Z*)-VP, must originate from a kinetic preference for the unlike intermediates or transition structures (ul-**I1**−**4** and ul-**TS1**−**3**, respectively).

Because intermediates **I1**−**3** depicted in Scheme 10 contain additional stereocenters on the bis-lactim moiety (R group), two different topologies can be present in either the like or unlike reaction channels. Thus, four diastereomeric pathways are possible depending on the face selectivity of both phosphonate carbanion SP and aldehyde. The initial transition structures were designated by a code of two letters in which the first label corresponds to the configuration of the former carbonyl carbon and the second is the configuration of the carbanion at the α-position. By extension, the like reaction channels giving rise to (*E*)-vinylphosphonate through (Re,Re) and (Si,Si) interactions were designated as RR and SS pathways, respectively, while the unlike channels giving rise to (*Z*)-vinylphosphonate through (Re,Si) and (Si,Re) interactions were designated as RS and SR pathways, respectively. For this study, we also have considered discrete solvation of the lithium with one or two THF molecules. The geometry optimizations were performed using a B3LYP DFT procedure with three different layers of basis set: 6-31G-(d)[32] for the critical parts of the reacting systems, 3-21G*[33] at the substituents to model steric effects, and the cc-pVDZ basis

(31) Gillies, M. B.; Tonder, J. E.; Tanner, D.; Norrby, P.-O. *J. Org. Chem.* **2002**, *67*, 7378−7388.

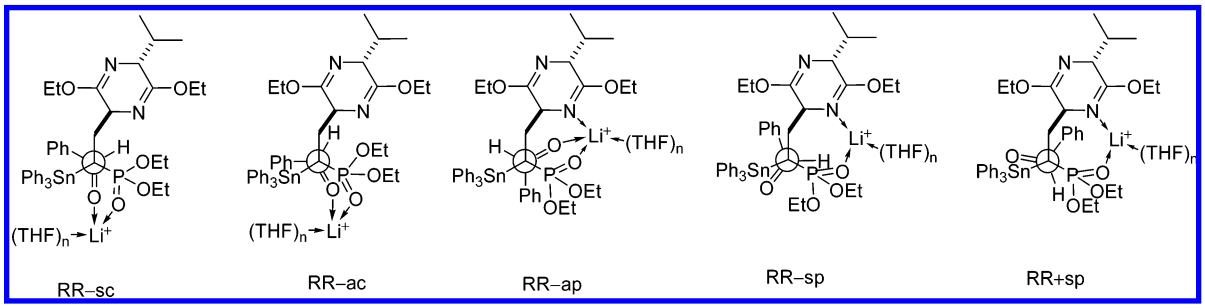

FIGURE 3. Synclinal (sc), anticlinal (ac), antiperiplanar (ap), and synperiplanar (sp) starting geometries for transition structure location in the RR diastereomeric pathway.

set[27] and a small-core relativistic pseudopotential (PP) for Sn[34] (see Computational Details in Supporting Information). Single point energy calculations also were performed at the B3LYP/cc-pVTZ-PP level both in the gas phase and of the bulk solvent effect in THF ($\epsilon = 7.52$) using Tomasi's PCM method.[29]

In the gas phase, addition of the phosphonate carbanion SP to benzaldehyde proceeds first by the exothermic formation of a disolvated lithium-coordinated complex dC (see Figure S4 of Supporting Information). Reorganization of this complex to the four possible 1,2-oxastannetanides *RR*-**I2**, *RS*-**I2**, *SR*-**I2**, and *SS*-**I2** was studied next. Five different families of starting geometries, which were characterized by a synperiplanar, synclinal, anticlinal, or antiperiplanar disposition of the carbonyl and triphenylstannyl moieties, were analyzed in each of the diastereomeric pathways (see Figure 3).

In the nucleophilic addition of the phosphonate carbanion to the carbonyl group, all the monosolvated transition structures were found to be higher in energy than the disolvated ones. In addition, most favorable transition structures arising from the synperiplanar geometries also were found to be higher in energy than those located by optimization of the antiperiplanar, anticlinal, and synclinal ones (see Table S4 of Supporting Information). The antiperiplanar transition structures (**TS1**-ap, see Figure S5 of Supporting Information) were calculated as the most stable ones and showed an energy gap of 2.0 kcal/mol between the like and the unlike reaction channels, which corresponded very well to experimental (*Z*)-preference. Nevertheless, these transition structures were expected to be nonproductive, as they led to antiperiplanar oxyanion intermediates (**I1**-ap) that had to surpass energy barriers of 11.6−22.7 kcal/mol for rotation around the new C−C bond to the synclinal geometries required for 1,2-oxastannetanide formation (see Figures S6 and S7 and additional discussion about torsional transition structures in Supporting Information). Conversely, the anticlinal and synclinal transition structures (**TS1**-sc and **TS1**-ac, see Figure 4) led to synclinal oxyanion intermediates (**I1**-sc, see Figure S8 of Supporting Information) which underwent direct cyclization to the corresponding 1,2-oxastannetanides without energy barriers for rotation around the P−C bond. Any attempts to localize transition structures for O−Sn bond formation (**TS2**) were unsuccessful in all the diastereomeric pathways.

According to the calculations, the synclinal and anticlinal transition structures (**TS1**-sc and **TS1**-ac) offered the lowest energy pathways for the 1,2-oxastannetanide formation with energy barriers of 7.7, 8.1, 9.9, and 10.3 kcal/mol in the SR, RS, RR, and SS pathways, respectively. In this manner, the initial C−C bond formation step favored unlike transition structures over the like counterparts. The most stable unlike transition structure, *SR*-**TS1**-sc, was 2.2 kcal/mol lower in energy than the most favorable transition structure in the like reaction channel, *RR*-**TS1**-sc. In *SR*-**TS1**-sc, the distance between the anionic oxygen and one of the triphenylstannyl hydrogens was 2.37 Å, which indicated a hydrogen bond interaction. This interaction was not possible for the like transition structures (*RR*-**TS1**-sc and *SS*-**TS1**-sc) and therefore could contribute to the energy difference between like and unlike reaction channels as previously reported in theoretical studies of the Horner−Wadsworth−Emmons olefinations.[35] This energy difference also could be derived from the steric repulsion in the like transition structures (see Figure 4). Thus, in *RR*-**TS1**-sc the distance between a hydrogen at the triphenylstannyl group and a carbon at the phenyl substituent of the aldehyde was 2.57 Å, which was less than the sum of their van der Waals radii (2.90 Å). Transition structures *SR*-**TS1**-sc and *RR*-**TS1**-sc lay in almost the same position along the reaction coordinate with a C−C bond forming distance of 2.30 Å and are characterized by synclinal N(1)C(2)C(1′)C(2′) angles and antiperiplanar C(2)C-(1′)C(2′)C(3′) angles.

Most stable 1,2-oxastannetanide intermediates showed a puckered ring where the tin atom is located over the plane of the three equatorial ligands,[36] while the lithium cation maintained a tetrahedral environment because of coordination to the oxygen atoms of the 1,2-oxastannetanide moiety, the phosphoryl group, and two THF molecules (see Figure S9 of Supporting Information). In the gas phase, the like 1,2-oxastannetanide intermediates *SS*-**I2** and *RR*-**I2** were calculated slightly lower in energy than the unlike isomers. The 1,2-oxastannetanide intermediates **I2** underwent cleavage of the C−Sn bond quite easily, with activation energies between 1.8 and 5.4 kcal/mol, to yield the phosphonate-stabilized carbanions **I3**. Transition structures **TS3** are relatively late with the C−Sn bond being weak at 3.00−3.20 Å (see Figure 5 and Figure S10 of Supporting Information). The most stable transition structure for C−Sn bond cleavage was located in the SR pathway, as was previously found for the 1,2-oxastannetanide formation. Thus, *SR*-**TS3** is calculated to be 2.1 kcal/mol lower in energy

(32) Francl, M. M.; Pietro, W. J.; Hehre, W. J.; Binkley, J. S.; Gordon, M. S.; DeFrees, D. J.; Pople, J. A. *J. Chem. Phys.* **1982**, *77*, 3654−3665.
(33) Binkley, J. S.; Pople, J. A.; Hehre, W. J. *J. Am. Chem. Soc.* **1980**, *102*, 939−947.
(34) Peterson, K. A. *J. Chem. Phys.* **2003**, *119*, 11099−11112.
(35) (a) Brandt, P.; Norrby, P.-O.; Martin, I.; Rein, T. *J. Org. Chem.* **1998**, *63*, 1280−1289. (b) For a recent theoretical evaluation of the binding energies of anions to simple arenes, see: Bryantsev, V. S.; Hay, B. P. *J. Am. Chem. Soc.* **2005**, *127*, 8282−8283.
(36) The X-ray crystallographic analysis of a pentacoordinated 1,2-oxastannnetanide has revealed a structure close to a square pyramid rather than a trigonal bipyramid. See: Kawashima, T.; Iwama, N.; Okazaki, R. *J. Am. Chem. Soc.* **1993**, *115*, 2507−2508.

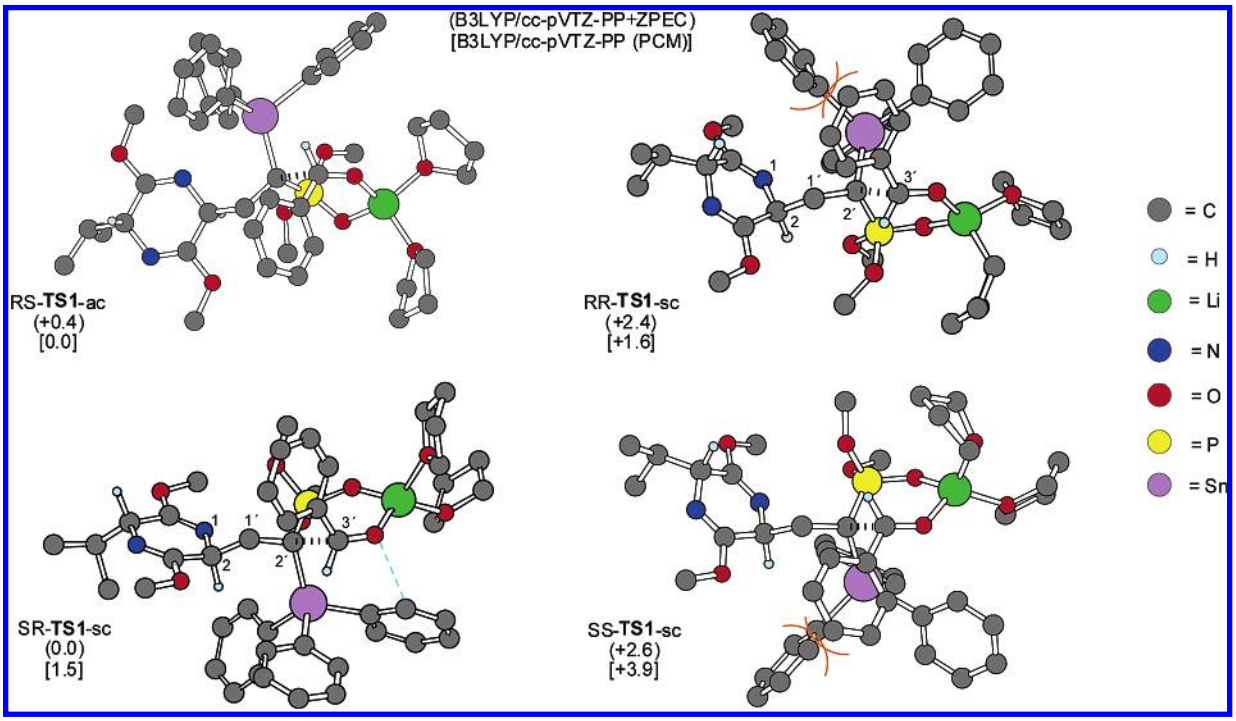

FIGURE 4. Chem3D representations for the most favored anticlinal or synclinal transition structures located (at B3LYP/6−31|3-21G(d)|PP level) for C−C bond formation in the tin−Peterson olefination. Relative energies in the gas phase (at B3LYP/cc-pVTZ-PP+ZPEC level) and in THF (at B3LYP/cc-pVTZ-PP (PCM) level) are shown in parentheses and brackets, respectively (kcal/mol). The hydrogen atoms are omitted for clarity except at chiral and prochiral centers.

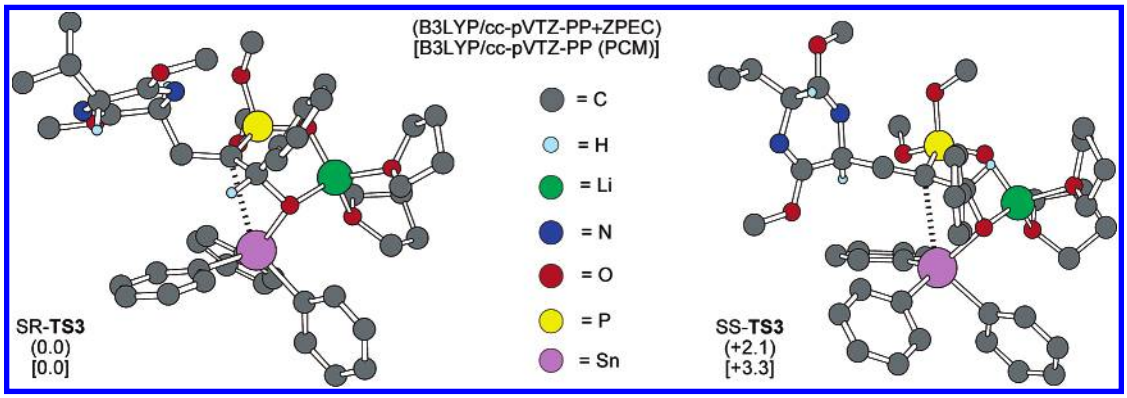

FIGURE 5. Chem3D representations for the most favored transition structures located (at B3LYP/6-31|3-21G(d)|PP level) for C−Sn bond cleavage of 1,2-oxastannetanide intermediates in the like and unlike reaction channels. Relative energies in the gas phase (at B3LYP/cc-pVTZ-PP+ZPEC level) and in THF (at B3LYP/cc-pVTZ-PP (PCM) level) are shown in parentheses and brackets, respectively (kcal/mol). The hydrogen atoms are omitted for clarity except at chiral centers.

than *SS*-**TS3**, which is the most stable transition structure in the like reaction channel.

Different from previous stationary points in the reaction profile, phosphonate-stabilized carbanion intermediates, transition structures for lithium stannoxide elimination, and final Z-vinylphosphonates were found to be lower in energy in the monosolvated series (**I3m**, **TS4m**, and **VPm**, respectively) than in the disolvated ones (**I3d**, **TS4d**, and **VPd**) (see Figures S11, S12, and S13 and Table S4 of Supporting Information). All the monosolvated geometries showed a four-coordinated cation because of the interaction of the lithium with a nitrogen (or oxygen) of the bis-lactim moiety and with the oxygen atoms of the phosphoryl group, the stannyloxy moiety, and one THF molecule. Thus, lithium coordination requirements in the monosolvated series determined bridged structures for **I3m** and **TS4m** and seven- or eight-membered chelate structures for **VPm** (see Figures 6, 7, and S13 of Supporting Information).

Formation of the phosphonate-stabilized intermediates **I3m** was calculated to be more exothermic than the preceding steps along the reaction path, and subsequent barriers to transition structures **TS4m** were relatively low (between 0.1 and 3.6 kcal/mol). The O−C bond to the triphenylstannyl group was weak at more than 1.5 Å in all the diastereomeric structures **I3m** (see Figure 6), as previously seen in related Peterson olefinations.[31] The lifetime of the intermediates **I3m** was likely to be short, therefore making the likehood of isomerization and potential loss of steric control because of C−C rotation fairly low. The monosolvated transition structure of lowest energy for the C−O

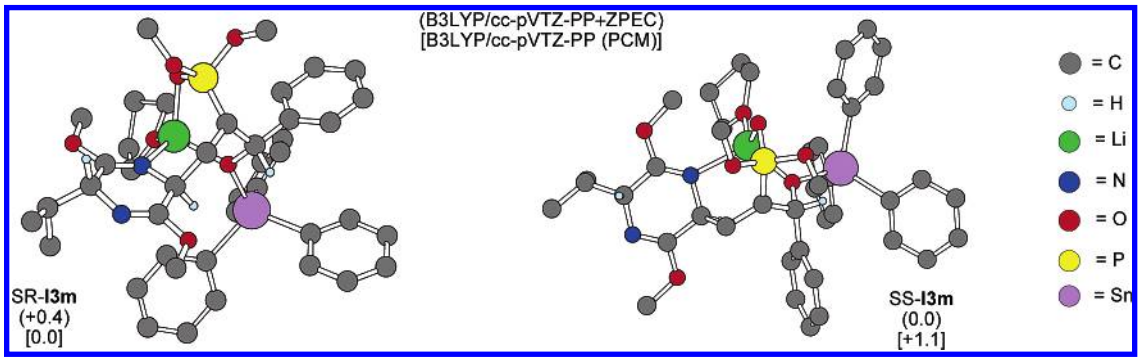

FIGURE 6. Chem3D representations for the most stable monosolvated phosphonate carbanion intermediates **I3m** located at B3LYP/6-31|3-21G-(d)|PP level. Relative energies in the gas phase (at B3LYP/cc-pVTZ-PP+ZPEC level) and in THF (at B3LYP/cc-pVTZ-PP (PCM) level) are shown in parentheses and brackets, respectively (kcal/mol). The hydrogen atoms are omitted for clarity except at chiral centers.

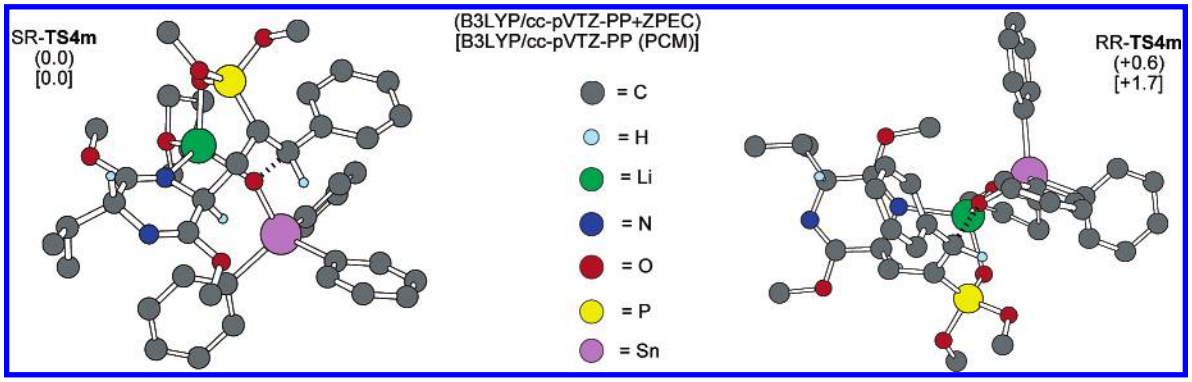

FIGURE 7. Chem3D representations for the most stable monosolvated transition structures **TS4m** located at B3LYP/6-31|3-21G(d)|PP level for the O−C bond cleavage. Relative energies in the gas phase (at B3LYP/cc-pVTZ-PP+ZPEC level) and in THF (at B3LYP/cc-pVTZ-PP (PCM) level) are shown in parentheses and brackets, respectively (kcal/mol). The hydrogen atoms are omitted for clarity, except at chiral centers.

bond cleavage was located again in the SR pathway, which was favored over the RR counterpart by 0.6 kcal/mol (see *SR*-**TS4m** and *RR*-**TS4m** in Figure 7). Finally, formation of vinylphosphonates **VPm** was computed to be highly exothermic. The main energetic features calculated in the gas phase for the four diastereomeric pathways are shown in the Figure 8.

The energetic profile for the tin−Peterson olefination in a dielectric medium simulating THF is shown in Figure 9. In solution, the activation energy for the initial C−C bond formation was reduced by more than 1.5 kcal/mol in the most favored like and unlike pathways. Thus, nonspecific solvation effects facilitated the rate-determining step but maintained the (*Z*)-selective course of the olefination. Nonspecific solvation of the transition structures **TS3** (with less charge-localized geometries) were less exothermic than for the 1,2-oxastannetanide intermediate **I2**, thus increasing the activation energies for the C−Sn bond cleavage by more than 2.0 kcal/mol. Differential nonspecific solvation effects on the competitive transition structures for C−Sn and C−O bond cleavage were markedly different. (*Z*)-Selectivity for the C−Sn bond cleavage in solution was increased by more than 1.2 kcal/mol, while the energy gap between the like and unlike pathways for C−O bond cleavage almost vanished in THF solution.

In summary, in accordance to DFT calculations, the tin−Peterson olefination of α-stannyl-stabilized phosphonate carbanions proceeded through an initial addition to the carbonyl group, followed by 1,2-oxastannnetanide formation, carbon−tin bond cleavage, and then carbon−oxygen cleavage. Computations indicated that rate and selectivity were determined in the initial carbon−carbon bond formation step in which the synclinal transition structures leading to (*Z*)-vinylphosphonates were favored by more than 1.4 kcal/mol, in accordance with experiment.

Transformation of the Substituted Bis-lactim Ethers into AP4 Derivatives. After separation of the mixtures of substitution or olefination products by chromatography, the 2′-substituted bis-lactim ethers **12ae**−**ak**, **13ae**,**af**,**ah**−**ak**, **14ai**, **23am**−**aq**, **24am**, **25**, and **26**, the 1′,2′-disubstituted bis-lactim ethers **19mb**, **20mb**,**nb**, **21mb**,**nb**, and **22mb**,**nb**, and the 2′,2′-difluorinated bis-lactim ether **16ae** could be isolated with diastereomeric excesses (de) higher than 98%. Conversion of the substituted bis-lactim ethers into the desired 2-amino-4-phosphonobutanoic acid derivatives was straightforward. Mild acid hydrolysis of 2′-substituted bis-lactim ethers **12ab/13ab**, **12ae**−**ag**,**ai**−**ak**, and **13ae**,**ai**−**ak** provided the corresponding 2,4-syn or 2,4-anti amino esters **27ab**,**ae**−**ag**,**ai**−**ak** and **31ab**,**ae**,**af**,**ai**−**ak** in high yields after the removal of the valine ester by chromatography (see Scheme 11). Subjecting the vinylphosphonates **23am**−**ap** and **24am** to the same reaction conditions furnished the (4*Z*)- or (4*E*)-amino esters **27am**−**ap** and **31am** (Scheme 12). In an analogous manner, hydrolysis of the 2′,2′-difluorinated bis-lactim ether **16ae** and the 1′,2′-disubstituted bis-lactims ethers **19mb**, **20mb**,**nb**, **21mb**,**nb**, and **22mb**,**nb** afforded the 4,4-difluorinated amino ester **33ae** and the 3,4-disubstituted amino esters **35mb**, **37mb**,**nb**, **39mb**,**nb**, and **41mb**,**nb** (Scheme 13).

Hydrolysis of the amino esters **27ab**,**ae**,**ag**,**ak**,**am**,**an**, **31ab**,-**ae**,**ak**,**am**, **33ae**, **35mb**, **37mb**,**nb**, **39mb**,**nb**, and **41mb**,**nb** to the corresponding amino acids **28ab**,**ae**,**ag***,**ak**,**am**,**an**, **32ab**,-

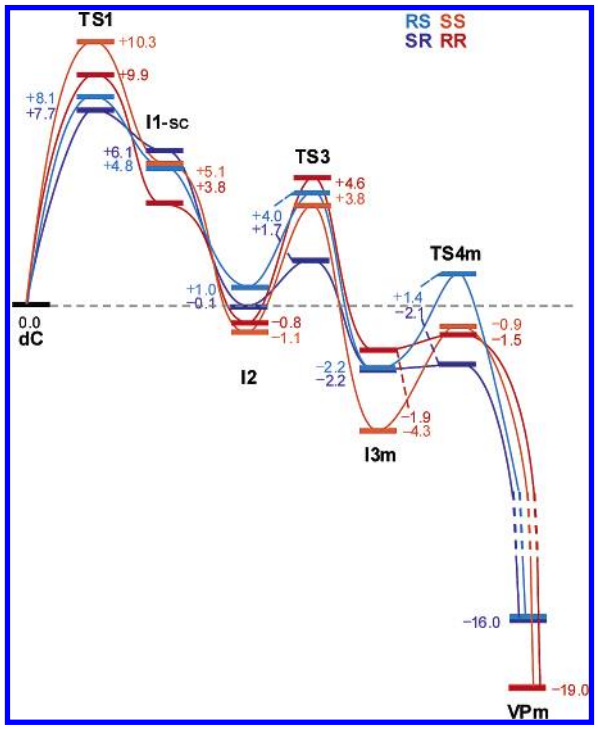

FIGURE 8. Energy profile for the tin−Peterson olefination in the gas phase. B3LYP/cc-pVTZ-PP+ZPEC energies relative to the disolvated complex **dC** are in kcal/mol. Color code for the diastereomeric pathways: SR-blue; RS-turquoise; RR-red; SS-orange.

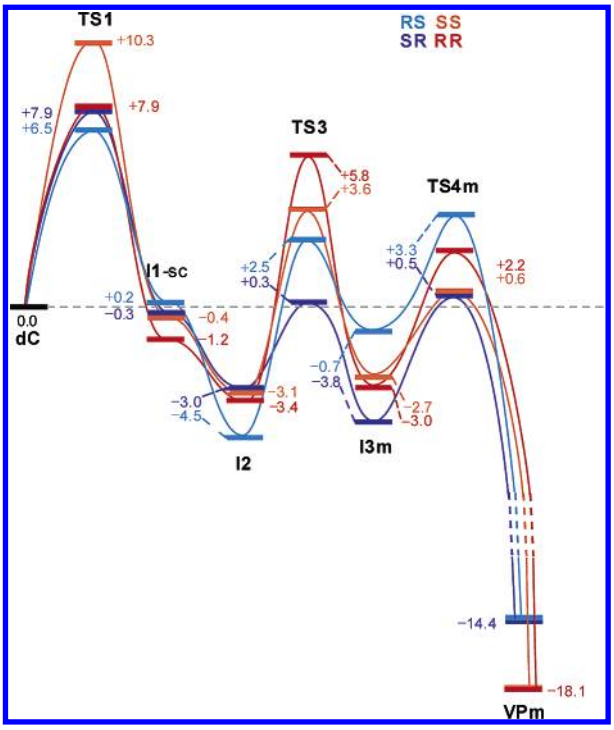

FIGURE 9. Energy profile for the tin−Peterson olefination in THF. B3LYP/cc-pVTZ-PP (PCM) free energies relative to the disolvated complex **dC** are in kcal/mol. Color code for the diastereomeric pathways: SR-blue; RS-turquoise; RR-red; SS-orange.

ae,**ak**,**am**, **34ae**, **36mb**, **38mb**,**nb**, **40mb**,**nb**, and **42mb**,**nb** was accomplished by heating in concentrated hydrochloric acid. In the same conditions, amino ester **27af** afforded a 3:1 mixture of amino acid **28af** and lactone **30af**. Upon crystallization from water, amino acid **32ak** yielded crystals amenable to X-ray structure determination, which allowed the confirmation of its 2,4-anti stereochemistry (see Supplementary Information). Hydrolysis of trimethylsilyl and azido substituted amino esters **27ai**,**aj** and **31ai**,**aj** required a treatment with trimethylsilyl bromide to yield the phosphonic acid intermediates **29ai**,**aj** and **33ai**,**aj**, which were subsequently hydrolyzed to the corresponding amino acids **28ai**,**aj** and **32ai**,**aj** with lithium hydroxide. Under these conditions, the thienyl-substituted amino ester **27ao** underwent complete isomerization of the olefinic double bond to afford the (4*E*)-vinylphosphonic acid **32ao**. After purification by reversed phase chromatography, mono- and disubstituted AP4 derivatives in the 2,4-anti, 2,4-syn, (4*Z*)-, and (4*E*)-series were isolated in high yields.

The formylated bis-lactim ethers **12ac** and **13ac** were stirred in 0.25 M hydrochloric acid under a hydrogen atmosphere and a palladium catalyst that enabled an intramolecular reductive

SCHEME 11[a]

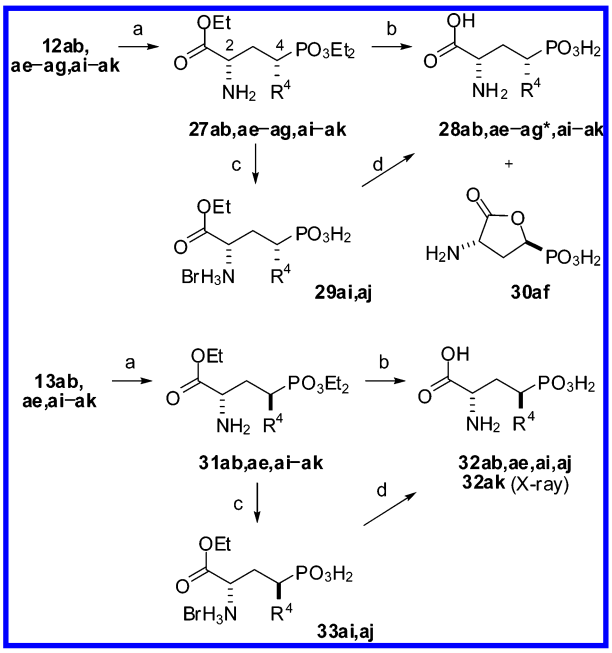

[a] Reagents and conditions: (a) 0.25 N HCl, THF, rt, 0.5−15 h (72−94%); (b) 12 N HCl, reflux, 2.5−8 h (83−100%); (c) (i) (TMS)Br, CH_2Cl_2, rt, 38 h; (ii) MeOH (67−100%); (d) (i) LiOH, H_2O, rt, 1 h; (ii) Dowex-H^+, H_2O (76−100%) Legend: **b**, R^4 = Me; **e**, R^4 = F; **f**, R^4 = OH; **g**, R^4 = PO_3Et_2; **g***, R^4 = PO_3H_2; **i**, R^4 = $SiMe_3$; **j**, R^4 = N_3; **k**, R^4 = Bn.

SCHEME 12[a]

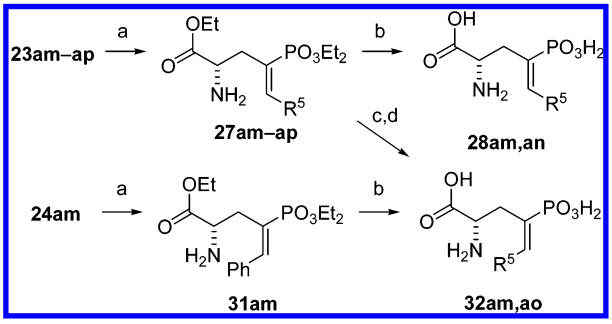

[a] Reagents and conditions: (a) 0.25 N HCl, THF, rt, 1−5 h (75−90%); (b) 12 N HCl, reflux, 3 h (63−83%); (c) (i) (TMS)Br, CH_2Cl_2, rt, 38 h; (ii) MeOH; (d) (i) LiOH, H_2O, rt, 1 h; (ii) Dowex-H^+, H_2O (94%). Legend: **m**, R^5 = Ph; **n**, R^5 = *i*-Pr; **o**, R^5 = 2-C_4H_3S; **p**, R^5 = CHCHPh.

SCHEME 13[a]

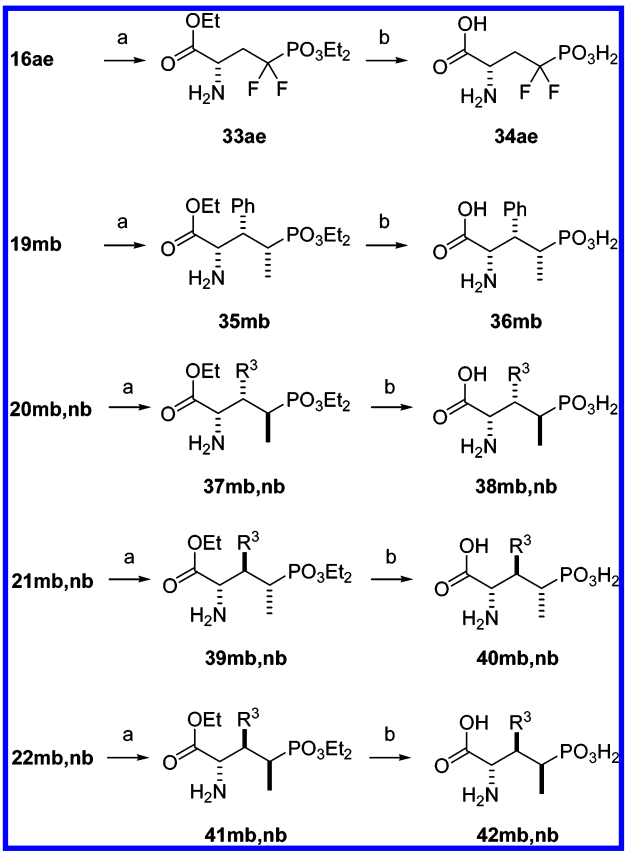

[a] Reagents and conditions: (a) 0.25 N HCl, THF, rt, 1−40 h (78−90%); (b) 12 N HCl, reflux, 2.5−10 h (80−96%). Legend: **m**, R^3 = Ph; **n**, R^3 = *i*-Pr.

amination after the hydrolysis of the pyrazine ring which led to a 8:1 mixture of the proline esters **27ac** and **31ac** (Scheme 14). Hydrolysis of **27ac** and **31ac** was accomplished by heating in 12 N HCl for 6 h, which gave a 8:1 mixture of 2,4-cis and 2,4-trans phosphonoprolines **28ac** and **32ac**. Catalytic hydrogenation of α-azidophosphonic acid[37] **28aj** gave the corresponding α-aminophosphonic acid **28ar**, which led to lactam **30ar** in excellent yield by heating in aqueous ammonia.

Determination of the Relative Configurations. Evidence supporting the relative configurations of the substitution and olefination products was obtained by NMR analyses. For compounds **12ab**,**ae**,**ag**,**ai**,**aj**, **13ab**,**ae**,**af**,**ah**−**aj**, **16ae**, **19mb**, **20mb**,**nb**, **21mb**, **22mb**, **23an**−**aq**, and **24am**, H-5 resonance appeared between 2.94 and 3.98 ppm as a triplet with $^5J_{H2H5}$ close to 3.5 Hz, which is general of the trans relationship of substituents at the pyrazine ring. The configurations of the vinylphosphonate moiety in the bis-lactim ethers were assigned on the basis of the $^3J_{HP}$ and the $^3J_{CP}$ observed in the ^{1}H and ^{13}C NMR spectra because of the coupling of H-3′ and C-4′ with the phosphorus atom at β−position. Thus, for **23am**−**ap** (see Scheme 7), $^3J_{H3'-P}$ (trans) values ranged from 44.4 to 49.3 Hz and $^3J_{C4'-P}$ (cis) values ranged from 7.8 to 12.1 Hz, which are characteristic for the vinylphosphonates with a (*Z*)-configuration. Conversely, for **24am** with an (*E*)-configuration, $^3J_{H3'-P}$ (cis) = 24.9 Hz and $^3J_{C4'-P}$ (trans) = 23.1 Hz.[38] Absolute configurations followed from the use of bis-lactim ethers derived from L- and D-Val as there is ample precedent.[39]

(37) Hanessian, S.; Bennani, Y. L. *Synthesis* **1994**, 1272−1274.

SCHEME 14[a]

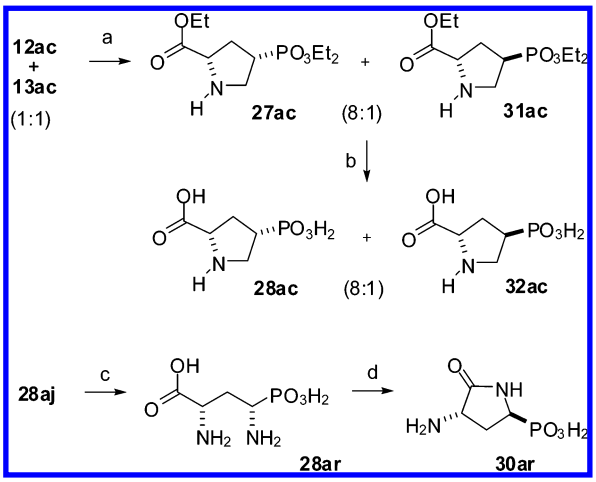

[a] Reagents and conditions: (a) 0.1 N HCl, H_2 (1 atm), Pd/C, rt, 3 h (69%); (b) 12 N HCl, reflux, 6 h (83%); (c) H_2 (1 atm), PtO_2, H_2O, rt, 16 h (90%); (d) NH_4OH, reflux, 24 h (94%).

Because none of the bis-lactim ethers, esters, or amino acids (other than **21mb** and **32ak**) provided crystals suitable for X-ray crystal structure determination, cyclic derivatives were sought that could enable the assignment of the relative configurations by NOESY. Six-membered amino-oxaphosphorinane derivatives were attractive because of the strong preference for the chair conformation reported for several substituted systems.[40] Conversion of amino esters **27ab**,**ae**, **31ab**,**ae**, **37mb**,**nb**, and **41nb** into such cyclic derivatives was achieved according to Scheme 15, by extending the applicability of previously developed methodology.[12] Chemoselective reduction of the carboxylic ester in the presence of the phosphonate was accomplished on the *N*-Boc derivatives of amino esters **43ab**,**ae**, **47ab**,**ae**, **51mb**,**nb**, and **54nb** by employing lithium borohydride in THF at room temperature. Reduction of 4-methyl-*N*-Boc-aminoesters **43ab** and **47ab** under these conditions were complete in 4 h and, after the mixtures of reduction were subjected to quench with methanol, workup, and chromatography, alcohols **44ab** and **48ab** could be isolated in high yields. Moreover, when the mixtures of reduction were stirred 68 h further at room temperature, cyclization of the intermediates were observed to afford the *N*-Boc-amino-oxaphosphorinanes **45ab** and **49ab** as single diastereoisomers at the phosphorus center. Cyclization of the intermediates in the reduction of 4-fluoro-*N*-Boc-amino esters **43ae** and **47ae** required only 8 h and gave the corresponding *N*-Boc-amino-oxaphosphorinanes **45ae** and **49ae** as 1:1 and 3:1 mixtures of epimers, respectively. In the same conditions, reduction and cyclization of the 3,4-disubstituted-*N*-Boc amino esters **51mb**,**nb** and **54nb** were complete in 20 h and furnished the corresponding *N*-Boc-amino-oxaphosphori-

(38) (a) Gorenstein, D. G. *Prog. Nucl. Magn. Reson. Spectrosc.* **1983**, *16*, 1−98. (b) *Phosphorus-31 NMR Spectral Properties in Compound Characterization and Structural Analysis;* Quin, L. D.; Verkade, J. G., Eds.; Wiley: New York, 1994.

(39) Schöllkopf, U.; Kühnle, W.; Egert, E.; Dyrbusch, M. *Angew. Chem., Int. Ed. Engl.* **1987**, *26*, 480−482.

(40) (a) Harvey, T. C.; Simiand, C.; Weiler, L.; Withers, S. G. *J. Org. Chem.* **1997**, *62*, 6722−6725. (b) Berkowitz, D. B.; Eggen, M.-J.; Shen, Q.; Shoemaker, R. K. *J. Org. Chem.* **1996**, *61*, 4666−4675. (c) Tasz, M. K.; Rodriguez, O. P.; Cremer, S. E.; Hussain, M. S.; Mazhar-ul-Haque *J. Chem. Soc., Perkin Trans. 2* **1996**, 2221−2226. (d) Lane, T. M.; Rodriguez, O. P.; Cremer, S. E.; Bennett, D. W. *Phosphorus, Sulfur Silicon Relat. Elem.* **1995**, *103*, 63−75. (e) Bergesen, K.; Vikane, T. *Acta Chem. Scand.* **1972**, *26*, 1794−1798. See also references 11.

SCHEME 15[a]

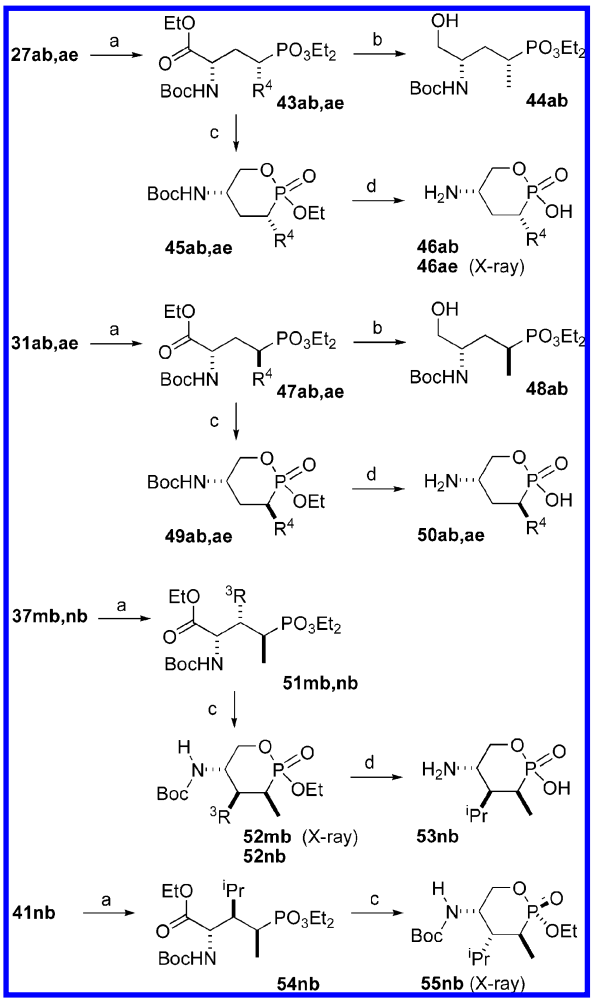

[a] (a) $(Boc)_2O$, $NaHCO_3$, Na_2CO_3, dioxane/H_2O 1:1, rt, 2−7 h (83−96%); (b) (i) 1.5 $LiBH_4$, THF, rt, 4 h; (ii) MeOH (90 or 93%); (c) (i) 1.5 $LiBH_4$, THF, rt, 8−72 h; (ii) MeOH (63−99%); (d) (i) TMSBr, CH_2Cl_2, rt, 15−27 h; (ii) MeOH (82−92%). Legend: **b**, R^4 = Me; **e**, R^4 = F; **m**, R^3 = Ph; **n**, R^3 = *i*-Pr.

nanes **52mb**,**nb** and **55nb** as single diastereoisomers at the phosphorus center. The *N*-Boc and *O*-ethyl ester groups of intermediates **45ab**,**ae**, **49ab**,**ae**, and **52nb** were cleaved with trimethylsilyl bromide in CH_2Cl_2 at room temperature to give the aminooxaphosphorinanes **46ab**,**ae**, **50ab**,**ae**, and **53nb** as pure diastereoisomers. Crystallization of **46ae** and **52mb** (from water) and **55nb** (from hexanes) yielded crystals amenable to X-ray structure determination, which allowed the confirmation of their relative configurations (see Supporting Information).

A single chair conformation was observed for oxaphosphorinanes **46ab** and **53nb** in the ^1H NMR spectra. These compounds, pyrrolidine **28ac**, and lactam **30ar** showed patterns of signals suitable for the study of their relative stereochemistry by NOESY. After we corroborated the ^1H NMR assignments by COSY experiments, the analysis of the sets of observed NOEs allowed the assignment of the relative configuration of the stereogenic centers formed in the electrophilic substitution. Thus, stereochemistry of pyrrolidine **28ac** was determined as 2,4-cis, while lactam **30ar** and oxaphosphorinane **46ab** showed 3,5-trans and 3,5-cis configuration, respectively. A 3,4-cis-4,5-trans configuration also was concluded for oxaphosphorinane **53nb**. The observed NOEs were supported by PM3/COSMO

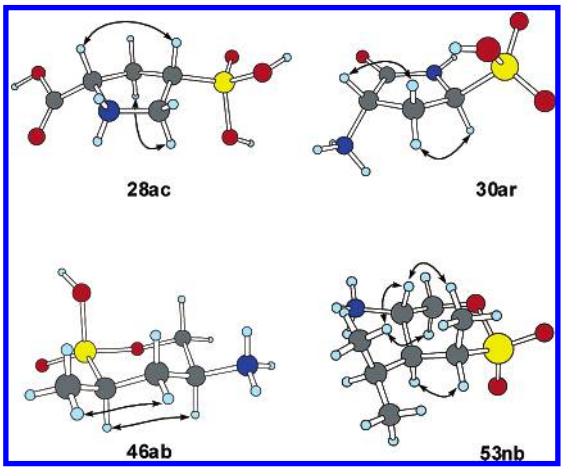

FIGURE 10. PM3/COSMO-optimized geometries for cyclic derivatives, showing characteristic NOEs.

semiempirical calculations.[41] The refined geometries for the cyclic derivatives in a polarizable dielectric continuum (simulating water or chloroform) were in agreement with the conformations in solution deduced from NMR spectroscopy, as depicted in Figure 10.

Conclusion

The electrophilic substitutions of lithiated bis-lactim ethers derived from *cyclo*-[L-AP4-D-Val] took place regioselectively α to the phosphonate group with a variable level of stereoselection depending on the nature of the electrophilic reagent and the pattern of substitution at the *β*-position. DFT calculations suggested that the stereoselectivity in these substitutions may have originated from the intervention of seven- and eight-membered lithium chelate structures. In THF solution, these intermediates preferentially adopt compact conformations (with higher dipole moments) in which the bis-lactim ether moiety effectively shields one of the faces of the carbanionic carbon and furnishes facial bias in the substitution. The olefination of benzaldehyde with α-silyl-, α-phosphoryl- and α−stannyl-stabilized phosphonate carbanions derived from *cyclo*-[L-AP4-D-Val] took place without compromising the chiral integrity of the bis-lactim ether, giving rise to vinylphosphonates with a different level of (*Z*)-stereoselection. In addition, the tin−Peterson reactions of the α-triphenylstannylphosphonate carbanion with structurally diverse carbonyl compounds were found completely (*Z*)-stereoselective. According to DFT calculations, this olefination proceeded with a stepwise mechanism through an initial nucleophilic addition of the phosphonate carbanion to the carbonyl group, followed by 1,2-oxastannnetanide formation, carbon−tin bond cleavage, and then carbon−oxygen cleavage. Computations indicated that rate and selectivity were determined in the initial carbon−carbon bond formation step in which the transition structures leading to (*Z*)-vinylphosphonates were favored by more than 1.4 kcal/mol. Finally, both the electrophilic substitutions and the tin−Peterson olefinations of lithiated bis-lactim ethers derived from *cyclo*-[L-AP4-D-Val] have been shown as a convenient approach to a variety of 4-substituted and 3,4-disubstituted 2-amino-4-phosphonobu-

(41) (a) PM3: Stewart, J. J. P. *J. Comput. Chem.* **1989**, *10*, 209−220, and 221−264. (b) COSMO: Klamt, A.; Schüürmann, G. *J. Chem. Soc., Perkin Trans. 2* **1993**, 799−805.

tanoic acids in enantiomerically pure form that may be useful tools for the study of group III of mGluRs.

Experimental Section

General Procedure for the Electrophilic Substitution on Li^+11aa$^-$. A solution of **11aa** (0.72 g, 1.92 mmol) in THF (8 mL) was added dropwise to a stirred solution of LDA (2.4 mmol) in THF (20 mL) at −78 °C, and the mixture was stirred for 15 min. Then a solution of the electrophilic reagent (2.3 mmol) in THF (2 mL) was added dropwise, the mixture was stirred for 5 min, and the reaction was quenched with AcOH or H_2O (10% in THF). The crude reaction mixture was warmed to room temperature, and the solvent was removed in vacuo. The resulting material was diluted with water and extracted with EtOAc. The combined organic layers were dried (Na_2SO_4) and evaporated, and the residue was purified by gradient flash chromatography to yield substitution products as colorless oils.

Fluoration of 11aa. Method A. General procedure was followed using 2 equiv of LDA (4.8 mmol) and *N*-fluorobenzenesulfonimide (NFSi) as the electrophilic reagent. The crude material was purified by flash chromatography (silica gel, EtOAc/hexanes 1:1 ratio) to give 0.55 g (ca. 72%) of a mixture of bis-lactims **12ae/13ae/16ae** in an 8.2:2.7:1.0 ratio. Method B. General procedure was followed using 2 equiv of NFSi (1.32 g, 4.00 mmol) as an electrophilic reagent. The crude material was worked up as described in method A to give 0.55 g (72%) of a mixture of bis-lactims **12ae/13ae/16a** in a 3:1:3 ratio. Method C. A solution of LDA (4.8 mmol) in THF (20 mL) was added dropwise to a solution of **11aa** (1.92 mmol) and NFSi (0.63 g, 1.92 mmol) in THF (15 mL) at −78 °C. After being stirred at −78 °C for 5 min, the reaction was quenched with AcOH (10% in THF) and worked up as described in method A to give 0.14 g of **11aa** (20%) along with 0.49 g (65%) of a mixture of bis-lactims **12ae/13ae** in a 3:1 ratio. Separation of the components of this mixture was accomplished by flash chromatography (silica gel, EtOAc/hexanes, from 1:4 to 2:1 ratio).

Data for (2*S*,5*R*,2′*S*)-3,6-diethoxy-2-[2-(diethoxyphosphoryl)-2-fluoroethyl]-2,5-dihydro-5-isopropylpyrazine (**12ae**): colorless oil; $[\alpha]_D^{26}$ −21.6 (c 2.9, CH_2Cl_2); IR (film) ν 1685 (C═N), 1235 (P═O), 1025 (POC) cm^{-1}; ^1H NMR ($CDCl_3$) δ 0.72 (d, J = 6.9 Hz, 3H), 1.02 (d, J = 6.9 Hz, 3H), 1.22−1.39 (m, 12H), 1.72 (m, 1H), 2.22 (dsp, J = 6.9, 3.4 Hz, 1H), 2.65 (m, 1H), 3.92 (t, J = 3.4 Hz, 1H), 4.00−4.30 (m, 9H), 5.34 (ddt, J = 47.0, 12.0, 1.5 Hz, 1H); ^{13}C NMR ($CDCl_3$) δ 14.1 (CH_3), 16.3 (d, J = 4.5 Hz, CH_3), 16.9 (CH_3), 18.9 (CH_3), 32.0 (CH), 35.1 (dd, J = 20.0, 2.7 Hz, CH_2), 50.4 (dd, J = 14.0, 2.7 Hz, CH), 60.5 (CH_2), 60.6 (CH_2), 60.7 (CH), 62.9 (d, J = 6.5 Hz, CH_2), 63.2 (d, J = 6.5 Hz, CH_2), 85.3 (dd, J = 179.0, 172.0 Hz, CH), 162.5 (C), 163.3 (C); ^{31}P NMR ($CDCl_3$) δ 19.6 (d, J = 74.3 Hz); ^{19}F NMR ($CDCl_3$) δ −213.7 (d, J = 74.3 Hz); FABMS (thioglycerol) m/z 396 ((M + 2)$^+$, 23), 395 (MH^+, 100). Anal. Calcd for $C_{17}H_{32}FN_2O_5P$: C, 51.77; H, 8.18; N, 7.10. Found: C, 51.85; H, 8.01; N, 7.38.

Data for (2*S*,5*R*,2′*R*)-3,6-diethoxy-2-[2-(diethoxyphosphoryl)-2-fluoroethyl]-2,5-dihydro-5-isopropylpyrazine (**13ae**): colorless oil; $[\alpha]_D^{22}$ +6.7 (c 0.8, CH_2Cl_2); IR (film) ν 1685 (C═N), 1235 (P═O), 1025 (POC) cm^{-1}; ^1H NMR ($CDCl_3$) δ 0.72 (d, J = 6.8 Hz, 3H), 1.02 (d, J = 6.9 Hz, 3H), 1.24−1.39 (m, 12H), 2.13−2.64 (m, 3H), 3.95 (t, J = 3.4 Hz, 1H), 4.00−4.30 (m, 9H), 5.03 (ddt, J = 47.0, 10.0, 3.4 Hz, 1H); ^{13}C NMR ($CDCl_3$) δ 14.1 (CH_3), 14.3 (CH_3), 16.3 (d, J = 6.0 Hz, CH_3), 16.6 (CH_3), 18.9 (CH_3), 32.0 (CH), 34.4 (dd, J = 19.4, 2.7 Hz, CH_2), 55.5 (dd, J = 13.0, 3.0 Hz, CH), 60.6 (CH_2), 62.8 (d, J = 6.5 Hz, CH_2), 63.1 (d, J = 6.5 Hz, CH_2), 86.0 (dd, J = 179.4, 172.5 Hz, CH), 162.4 (C), 164.3 (C); ^{31}P NMR ($CDCl_3$) δ 19.0 (d, J = 74.7 Hz); ^{19}F NMR ($CDCl_3$) δ −212.2 (d, J = 74.8 Hz); FABMS (thioglycerol) m/z 396 ((M + 2)$^+$, 23), 395 (MH^+, 100). Anal. Calcd for $C_{17}H_{32}FN_2O_5P$: C, 51.77; H, 8.18; N, 7.10. Found: C, 51.96; H, 8.31; N, 7.07.

Data for (2*S*,5*R*)-3,6-diethoxy-2-[2-(diethoxyphosphoryl)-2,2-difluoroethyl]-2,5-dihydro-5-isopropylpyrazine (**16ae**): colorless oil; $[\alpha]_D^{26}$ −7.4 (c 2.4, CH_2Cl_2); IR (film) ν 1685 (C═N), 1225 (P═O), 1015 (POC) cm^{-1}; ^1H NMR ($CDCl_3$) δ 0.67 (d, J = 6.8 Hz, 3H), 0.99 (d, J = 6.9 Hz, 3H), 1.18−1.37 (m, 12H), 2.12−2.47 (m, 2 H), 2.70 (dtt, J = 27.3, 14.7, 3.5 Hz, 1H), 3.87 (t, J = 3.5 Hz, 1H), 4.00−4.38 (m, 9H); ^{13}C NMR ($CDCl_3$) δ 14.2 (CH_3), 16.3 (d, J = 5.6 Hz, CH_3), 16.7 (CH_3), 19.0 (CH_3), 31.7 (CH), 37.7 (dt, J = 19.2, 14.9 Hz, CH_2), 50.4 (t, J = 3.9 Hz, CH), 60.6 (CH), 60.7 (CH_2), 60.8 (CH_2), 64.4 (d, J = 6.4 Hz, CH_2), 121.0 (dt, J = 270.0, 216.0 Hz, C), 161.5 (C), 163.1 (C); ^{31}P NMR ($CDCl_3$) δ 7.4 (t, J = 107.0 Hz); ^{19}F NMR ($CDCl_3$) δ −110.6 (dd, J = 298.5, 107.0 Hz), −112.6 (dd, J = 298.5, 107.0 Hz); FABMS (thioglycerol) m/z 414 ((M + 2)$^+$, 20), 413 (MH^+, 100). Anal. Calcd for $C_{17}H_{31}F_2N_2O_5P$: C, 49.51; H, 7.58; N, 6.79. Found: C, 49.35; H, 7.41; N, 6.94.

Olefination of Bis-lactim Ethers Derived from *cyclo*-[L-AP4-D-Val]. General Procedure. A solution of **12/13ad,ah** or **12ag** (0.94 mmol) in THF (8 mL) was added dropwise to a stirred solution of LDA (1.22 mmol) in THF (30 mL) at −78 °C, and the mixture was stirred for 15 min. Then a solution of the carbonyl compound (1.12 mmol) in THF (2 mL) was added dropwise, and the reaction was slowly warmed to reach 0 °C after ca. 4 h. The reaction was quenched with AcOH (1.5 mmol, 10% in THF), the crude reaction mixture was warmed to room temperature, and the solvent was removed in vacuo. The resulting material was diluted with water and was extracted with EtOAc. The combined organic layers were dried (Na_2SO_4) and evaporated, and the residue was purified by gradient flash chromatography to yield olefination products as colorless oils.

Wadsworth−Horner−Emmons Benzylidenation. In accordance to the general procedure, the reaction of **12ag** (0.48 g) with benzaldehyde (0.11 mL) gave 0.34 g (77%) of a mixture of vinylphosphonates **23am/24am** in a 5:1 ratio and 48 mg (10%) of the starting compound after chromatography (silica gel, EtOAc/hexanes 1:2).

Tin−Peterson Benzylidenation. In accordance to the general procedure, the reaction of **12/13ah** (0.68 g) with benzaldehyde (0.11 mL) gave 0.24 g (56%) of bis-lactim **23am** and 0.17 g (25%) of the starting compound after chromatography (silica gel, EtOAc/hexanes 1:2).

Peterson Benzylidenation. A solution of *n*-BuLi (0.37 mL, 2.5 M in hexane, 1 equiv) was added to a stirred solution of (3*R*)-2,5-diethoxy-3-isopropyl-3,6-dihydropyrazine (0.20 g, 0.94 mmol) in THF (10 mL) at −78 °C, and the mixture was stirred for 30 min. Then, a solution of α-trimethylsilylvinylphosphonic acid diethyl ester (0.26 g, 1.15 equiv) in THF (5 mL) was added dropwise, and the mixture was stirred for 15 min. Then a solution of benzaldehyde (0.11 mL) in THF (2 mL) was added dropwise, and the reaction was slowly warmed to reach 0 °C after ca. 4 h. The reaction was quenched with AcOH (1.5 mmol, 10% in THF), the crude reaction mixture was warmed to room temperature, and the solvent was removed in vacuo. The resulting material was diluted with water and extracted with EtOAc. The combined organic layers were dried (Na_2SO_4) and evaporated, and the residue was purified by gradient flash chromatography to yield 0.31 g (70%) of a mixture of vinylphosphonates **23am/24am** in a 3:2 ratio and 46 mg (11%) of a mixture of **12/13ai**.

Data for (2*S*,5*R*,2′*Z*)-3,6-diethoxy-2-[2-(diethoxyphosphoryl)-3-phenylprop-2-enyl]-2,5-dihydro-5-isopropylpyrazine (**23am**): $[\alpha]_D^{20}$ −24.4 (c 1.1, CH_2Cl_2); IR (film) ν 1690 (C═N), 1235 (P═O), 1028 (POC) cm^{-1}; ^1H NMR ($CDCl_3$) δ 0.72 (d, J = 6.8 Hz, 3H), 1.07 (d, J = 6.8 Hz, 3H), 1.08 (t, J = 7.0 Hz, 3H), 1.09 (t, J = 7.0 Hz, 3H), 1.25 (t, J = 7.0 Hz, 3H), 1.29 (t, J = 7.0 Hz, 3H), 2.28 (dsp, J = 6.8, 3.4 Hz, 1H), 2.48 (ddd, J = 20.5, 14.6, 8.8 Hz, 1H), 3.17 (ddd, J = 14.2, 12.7, 4.4 Hz, 1H), 3.80−4.23 (m, 8H), 4.25−4.34 (m, 1H), 7.20 (d, J = 44.4 Hz, 1H), 7.27−7.51 (m, 5H); ^{13}C NMR ($CDCl_3$) δ 14.3 (CH_3), 15.9 (d, J = 7.1 Hz, CH_3), 16.7 (CH_3), 19.0 (CH_3), 31.6 (CH), 41.0 (d, J = 2.1 Hz, CH_2), 55.1 (d, J = 2.5 Hz, CH), 60.6 (CH), 60.6 (CH_2), 61.4 (d, J = 6.0 Hz, CH_2), 126.7 (d, J = 174.6 Hz, C), 127.6 (CH), 127.9 (CH), 128.9 (CH), 136.6

(d, J = 7.8 Hz, C), 147.0 (d, J = 7.9 Hz, CH), 162.8 (C), 162.9 (C); ^{31}P NMR ($CDCl_3$) δ 18.4; FABMS (thioglycerol) m/z 465 (MH^+, 100). Anal. Calcd for $C_{24}H_{37}N_2O_5P$: C, 62.05; H, 8.03; N, 6.03. Found: C, 61.74; H, 8.29; N, 6.16.

Data for (2*S*,5*R*,2′*E*)-3,6-diethoxy-2-[2-(diethoxyphosphoryl)-3-phenylprop-2-enyl]-2,5-dihydro-5-isopropylpyrazine (**24am**): $[\alpha]_D^{20}$ +141.9 (c 0.4, CH_2Cl_2); IR (film) ν 1690 (C═N), 1240 (P═O), 1035 (POC) cm^{-1}; ^{1}H NMR ($CDCl_3$) δ 0.75 (d, J = 6.8 Hz, 3H), 1.02 (d, J = 6.8 Hz, 3H), 1.17−1.38 (m, 12H), 2.21 (dsp, J = 6.8, 3.9 Hz, 1H), 2.48−3.08 (m, 2H), 3.91 (t, J = 3.4 Hz, 1H), 3.93−4.27 (m, 8H), 4.41−4.50 (m, 1H), 7.24−7.49 (m, 5H), 7.66 (d, J = 24.9 Hz, 1H); ^{13}C NMR ($CDCl_3$) δ 14.3 (CH_3), 16.3 (d, J = 5.3 Hz, CH_3), 17.0 (CH_3), 19.0 (CH_3), 32.1 (CH), 32.9 (d, J = 9.3 Hz, CH_2), 53.9 (CH), 60.5 (CH), 60.9 (CH_2), 61.7 (d, J = 7.0 Hz, CH_2), 61.9 (d, J = 7.0 Hz, CH_2), 127.3 (d, J = 174.2 Hz, C), 128.2 (CH), 129.2 (CH), 135.5 (J = 23.1 Hz, C), 145.5 (J = 11.7 Hz, CH), 163.1 (C), 163.5 (C); ^{31}P NMR ($CDCl_3$) δ 22.6; FABMS (thioglycerol) m/z 465 (MH^+, 100). Anal. Calcd for $C_{24}H_{37}N_2O_5P$: C, 62.05; H, 8.03; N, 6.03. Found: C, 62.39; H, 8.10; N, 6.31.

Acknowledgment. We gratefully acknowledge Ministerio de Ciencia y Tecnología (Spain) and the European Regional Development Fund (Projects BQU200-0236 and BQU2003-00692) and Xunta de Galicia (PGIDIT05BTF10301PR) for financial support, and Novartis Pharma for the generous gift of bis-lactim ethers derived from *cyclo*-[Val-Gly]. We also thank Dr. Miguel A. Maestro, Dr. Alberto Fernández, and Dr. Ana I. Balana for resolving the X-ray structures. The authors are indebted to Centro de Supercomputación de Galicia for providing the computer facilities. O.B. thanks Xunta de Galicia for an "Isidro Parga Pondal" position at Universidade da Coruña.

Supporting Information Available: Experimental procedures and full characterization of new compounds. Crystallographic data for compounds **21mb**, **32ak**, **46ae**, **52mb**, and **55nb**. Computational methods, Cartesian coordinates, and absolute energies for all the models reported. This material is available free of charge via the Internet at http://pubs.acs.org.

JO061072X